

Recent Advances in Dispersant Technology for Carbon Nanotubes toward Energy Device Applications

Yong Jun Choi, Edric John Cruz Nacpil, Jiye Han, Chunhong Zhu, Ick Soo Kim,* and Il Jeon*

Carbon nanotubes (CNTs) are of interest in various industries owing to their high aspect ratio, electrical conductivity, and other properties. By maximizing the number of CNTs in their solvents or matrices, the electrical and mechanical performance in applications such as batteries, sensors, and transistors can be enhanced. However, the hydrophobicity of CNTs' surface induces aggregation that adversely impacts their performance. To overcome this obstacle, many researchers have been designing novel dispersants with performances exceeding that of existing commercial dispersants. This article reviews contemporary studies on CNT dispersants from 2015 to 2022, along with the comprehensive features of CNTs depending on their chirality, number of walls, synthesis methods, and functionalization. Studies of CNT dispersants are primarily organized according to whether aqueous or organic solvents are used. This review article provides a clear perspective of CNT dispersants development today and how to design new CNT dispersants depending on the solvents. A conclusion is given to identify major challenges to the implementation of CNT dispersion and an outlook on future avenues of research.

1. Introduction

From the 20th century to the present, the development of advanced nanomaterials and their industrial applications in

nanotechnology has seen rapid growth.^[1] Among various nanomaterials, nanocarbons have become the focus of development. Allotropes of carbon, such as graphene,^[2] fullerene,^[3] carbon quantum dots,^[4] and carbon nanotubes (CNTs),^[5] have attracted considerable attention in the industry owing to their excellent mechanical and electrical properties.^[6–8] Among these materials, the development of fullerene and CNTs has advanced the closest to commercialization. The commercial deployment of CNTs has been particularly favored due to their large specific surface area, high aspect ratio,^[9,10] high electrical and thermal conductivities along the tube axis,^[11–13] and excellent mechanical and chemical stability.^[14,15] Such desirable characteristics have led to their deployment in applications such as lithium-ion battery anodes,^[16] electrochemical sensors,^[17] field-effect transistors,^[18] alter-

native electrodes,^[19] supercapacitors,^[20] hydrogen storage,^[21] and flexible electrochemical devices.^[22] However, a common challenge across scientific disciplines is the tendency for CNTs to aggregate.^[23] Aggregated CNTs dramatically reduce material performance^[24]; thus, scientists aim to optimize CNT dispersion as a countermeasure.^[25]

Recently, carbon neutrality policies, that is, net zero carbon emissions, have been implemented in most countries to reduce the use of fossil fuels, resulting in a significant demand for renewable energy. Nonetheless, due to the intermittent production of renewable energy, an energy storage system (ESS) is required.^[26] Furthermore, industries are striving to increase their battery capacity with the expanding usage of mobile phones, laptops, and electric vehicles. While many studies to increase battery capacity have been conducted, the current progress could be more extensive.^[27] To achieve meaningful advancements in battery capacity, many researchers have turned to the application of CNTs as cathode and anode materials.^[19,28–31] When used in small amounts, CNTs have been proven to increase the electrical conductivity of the cathodes.^[32–34] CNTs can replace conventional carbon black and graphite for anodes, which suffer from low performance and degrading overcharge/discharge cycles.^[35] Before widespread deployment of CNTs as cathode and anode materials can be realized, CNTs must overcome their aggregation issue, which stems from their poor dispersibility in solvents. Numerous methods have been reported to improve CNT

Y. J. Choi, E. J. C. Nacpil, J. Han, I. Jeon
Department of Nano Engineering
Department of Nano Science and Technology
KKU Advanced Institute of Nanotechnology (SAINT)
Sungkyunkwan University (SKKU)
Suwon 16419, Republic of Korea
E-mail: il.jeon@spc.oxon.org

C. Zhu, I. S. Kim, I. Jeon
Nano Fusion Technology Research Group
Institute for Fiber Engineering (IFES)
Interdisciplinary Cluster for Cutting Edge Research (ICCER)
Shinshu University
Tokida 3-15-1, Ueda, Nagano 386-8567, Japan
E-mail: kim@shinshu-u.ac.jp

 The ORCID identification number(s) for the author(s) of this article can be found under <https://doi.org/10.1002/aesr.202300219>.

© 2024 The Authors. Advanced Energy and Sustainability Research published by Wiley-VCH GmbH. This is an open access article under the terms of the Creative Commons Attribution License, which permits use, distribution and reproduction in any medium, provided the original work is properly cited.

DOI: [10.1002/aesr.202300219](https://doi.org/10.1002/aesr.202300219)

dispersibility in organic and aqueous solvents. So far, the dispersant-driven method is an effective and economical way of enhancing CNT solubility because synthesizing surfactants is economically favorable. Also, unlike chemical modification methods, there is little or no damage to the CNTs.

Despite the importance of CNT dispersion, there is a dearth of reviews that detail the state of CNT dispersants.^[36,37] Although research on CNT dispersants has continued to date, there has yet to be a comprehensive review of contemporary CNT dispersant technology. With the widespread push for the industrial application of CNTs, we provide a timely overview of the latest technologies for CNT dispersion. To begin, we present the fundamentals of CNTs in Section 2.1, which include the effects of chirality and architectures on the properties of CNTs. Other materials used energy device applications are compared to CNTs with respect to dispersibility. Section 2.2 introduces various CNT synthesis methods categorized according to their advantages and disadvantages. Section 3 details different approaches that improve the dispersibility of CNTs by mechanical modification, and covalent and noncovalent functionalization. Subsequently, we highlight the use of dispersants for CNT dispersibility enhancement. Dispersants are widely used in industry, particularly for electrical energy storage applications. As the core part of this review, Section 3.2 features dispersants for CNTs that are reported between 2015 and 2022. Section 3.2 is organized according to dispersants for aqueous and organic solvents, and their respective chemical features and dispersibility. Moreover, the use of such dispersants in energy devices is discussed in detail. Considering that there has yet to be a review of the application of CNT dispersants in energy devices, this review represents a milestone for industrial applications of dispersibility-enhanced nanocarbon materials using nanoscale dispersants.

2. Background

2.1. Fundamentals and Classification of CNTs

2.1.1. Chirality of CNTs

Gaining a rudimentary understanding of graphene assists in understanding the structure of CNTs. A single-walled CNT (SWCNT) is formed by connecting the edges of a graphene sheet, as shown in **Figure 1a**. Graphene has four valence bonds consisting of three σ (s , p_x , p_y) bonds and one π bond (p_z). The three strong covalent σ bonds form a planar sp^2 , and the remaining p_z orbitals become a manifold of delocalized π/π^* orbitals existing in the planes above and below the carbon sheet.^[38] In this regard, SWCNT has the same chemical bonding as graphene. However, due to the curvature, the mechanical and electrical properties of CNTs depend on which chiral vector the graphene sheet is reeled from during CNT formation. The chiral vector of a CNT is determined by the honeycomb lattice, leading to a defined structure. We express the vector as

$$\vec{C}_h = n\vec{a}_1 + m\vec{a}_2 = (n, m) \quad (1)$$

where n and m are positive integers, and n is $\leq m$.^[39] The type of CNT depends on the formation of the chiral vector. CNTs can be classified into two branches: achiral and chiral. The former has a

mirror surface that is wholly overlapped, and the latter cannot be superimposed on its mirror image. Achiral CNTs have either a zigzag form with a chiral vector $n = 0$ or an armchair form with $n = m$. The electrical properties of CNTs vary according to their symmetry.^[40,41] This means that the bandgap of each CNT is nonuniform because the carbon arrangements differ slightly from those of graphene. The zone-folding approximation demonstrates that CNTs are metallic or semiconducting. The wave function of a CNT in the Brillouin zone was set using Bloch's theorem to represent the periodic boundary conditions (Figure 1b).^[41] The quantization lines are then determined in the reciprocal space. The electrical properties of CNTs are determined based on whether the quantization lines are located on the Dirac points (Figure 1c).^[42] A law based on this mechanism determines whether CNTs are metallic or semiconducting. If $n - m = 3k$, where k is zero or a positive integer, the Fermi levels of metallic CNTs are located at Dirac points, whereas those of other CNTs are semiconducting. One-third of the existing CNTs are metallic, including all armchair CNTs, where $n - m = 0$ (Figure 1d,e).^[42,43]

2.1.2. CNT Architecture and Architectures of Alternative Materials

The feasibility of materials incorporated into energy devices varies according to properties of each material category and the target energy device. As CNTs possess dispersibility in solvents that is partly determined by architecture, CNTs are a versatile option for energy storage devices, such as batteries, and energy conversion devices, such as solar cells. Other materials, including graphene and MXene, also possess architectures lending to dispersibility in the fabrication of energy device such as solar cells.^[44,45] Consideration will be given at the end of this section to some alternative materials as a basis for comparing the dispersibility of CNTs.

Based on the number of nanotubes, CNTs are categorized as SWCNT (Figure 2a,d), double-walled CNT (DWCNT) (Figure 2e), or multiwalled CNT (MWCNT) (Figure 2b,c,f)).^[46,47] SWCNT and DWCNT consist of one and two layers of CNT, respectively. MWCNTs comprise three or more layers of CNT. Each CNT type has its unique characteristics. For example, SWCNTs have a lower optical density than either DWCNTs or MWCNTs, which is why they are commonly used as transparent conductors.^[48–51] The diameter and length distributions of CNTs are generally controlled by the synthesis conditions provided by the synthesis methods, catalysts, and temperature. CNTs with fewer walls are favored for energy device applications. In the case of battery applications, SWCNTs are preferred over MWCNTs for higher conductivity. At the same time, SWCNTs are favored in solar cell applications because of their lower optical density^[50,52] and suitable bandgap.^[53–55]

Table 1 lists the mechanical and electrical properties and costs of SWCNTs, DWCNTs, and MWCNTs. Rols et al.^[56] measured SWCNT distribution by reading the Raman-active A_{1g} radial-breathing mode frequency. It was found that the distributed diameter was between 1.24 and 1.95 nm. Bandow et al.^[57] synthesized SWCNTs via pulse laser vaporization using Fe/Ni and Co/Ni catalysts. The researchers controlled the growth temperature to narrow the distribution of SWCNT diameters to be

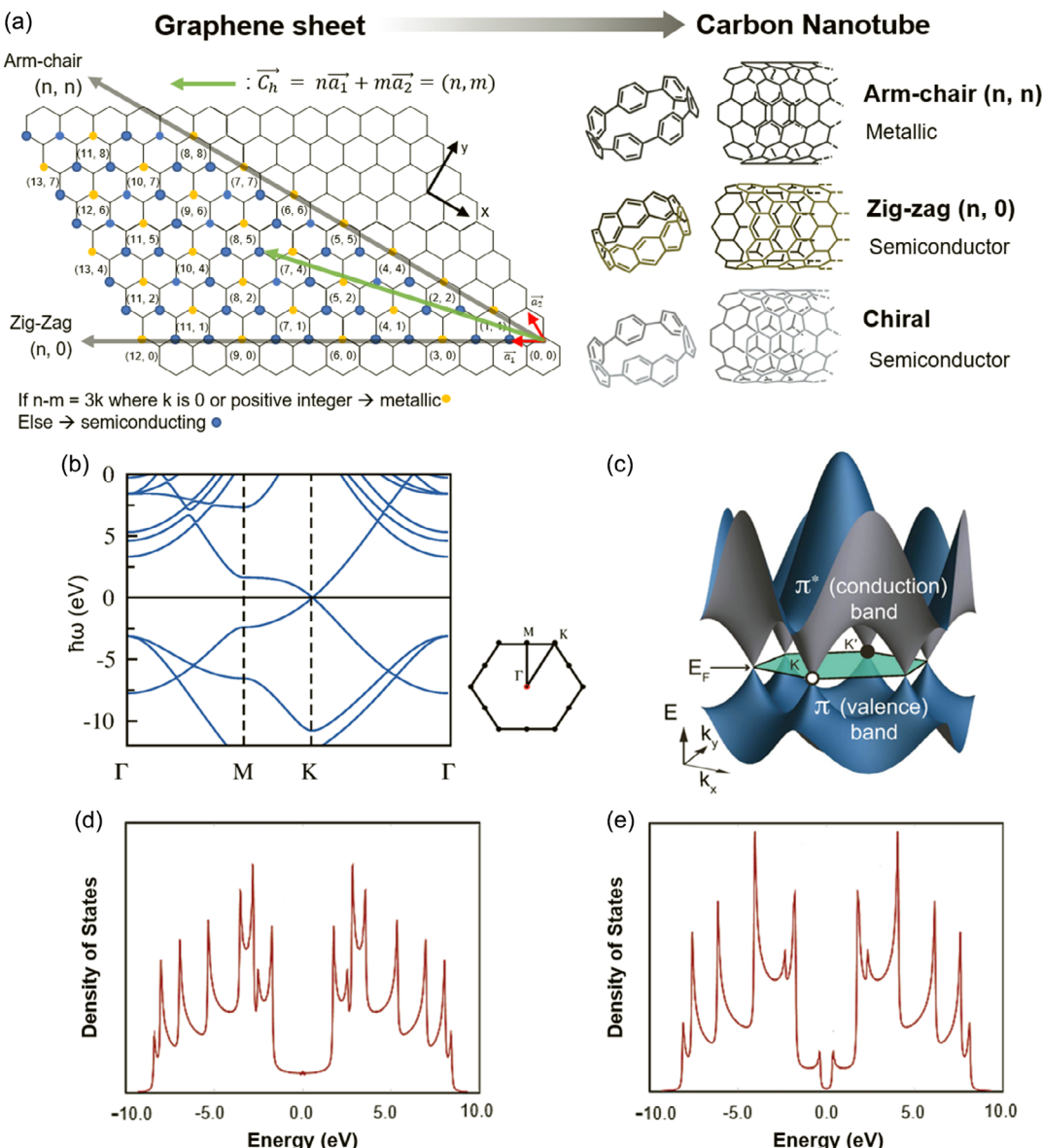


Figure 1. a) Classification of CNT structures depending on chiral vector, \vec{C}_h , expressed by chiral indices (n,m) and spanning a graphene sheet. Chiral indices determine electronic properties and CNT structures (arm-chair, zig-zag, and chiral structures). b) Band structure of graphene on Brillouin zone.^[41] c) 3D image of π band and π^* band on a graphene sheet. Two bands meet on six Dirac points in the first Brillouin zone. Reproduced with permission.^[42] Copyright 2015, American Physical Society. d,e) DOS image of arm-chair (5,5) CNT and zig-zag (7,0) CNT. Arm-chair (5,5) CNT shows metallic behavior due to charge carriers near Fermi energy. Due to no charge carriers at Fermi energy, zig-zag (7,0) CNT has semiconducting properties. Reproduced with permission.^[43] Copyright 2002, American Chemical Society.

between ≈ 0.81 and ≈ 1.51 nm. However, DWCNTs consist of inner and outer diameters that are noted separately. Using high-resolution transmission electron microscopy (HRTEM) and resonant Raman spectra to analyze the diameter of DWCNTs, Ren and Cheng^[58] measured inner and outer diameters to be between 1.0–1.3 and 1.7–2.0 nm, respectively. In another study, the mean values for inner and outer diameters were 0.85 and 1.55 nm, respectively.^[59] The mean lengths and specific surface areas (SSAs) were published in a commercially available dataset from Ossila, a CNT manufacturer.^[60] The

average lengths of the SWCNT powders (Ossila.com, M2013L1) were between 4 and 20 μm with a SSA between 400 and 1000 $\text{m}^2 \text{g}^{-1}$. Similarly, the average length and SSA of DWCNTs (Ossila.com, M2016L1) are $\approx 50 \mu\text{m}$ and $350 \text{ m}^2 \text{ g}^{-1}$, respectively, and those of MWCNTs (Ossila.com, M2008D1) are 10–30 μm and $> 500 \text{ m}^2 \text{ g}^{-1}$, respectively.

Dresselhaus and co-workers^[61] measured the tensile strength of SWCNTs to be 22.2 ± 2.2 GPa. Cheng et al.^[62] evaluated five samples of pristine DWCNTs with tensile strengths ranging from 51 to 84 GPa. Barber et al.^[63] computed Weibull–Poisson

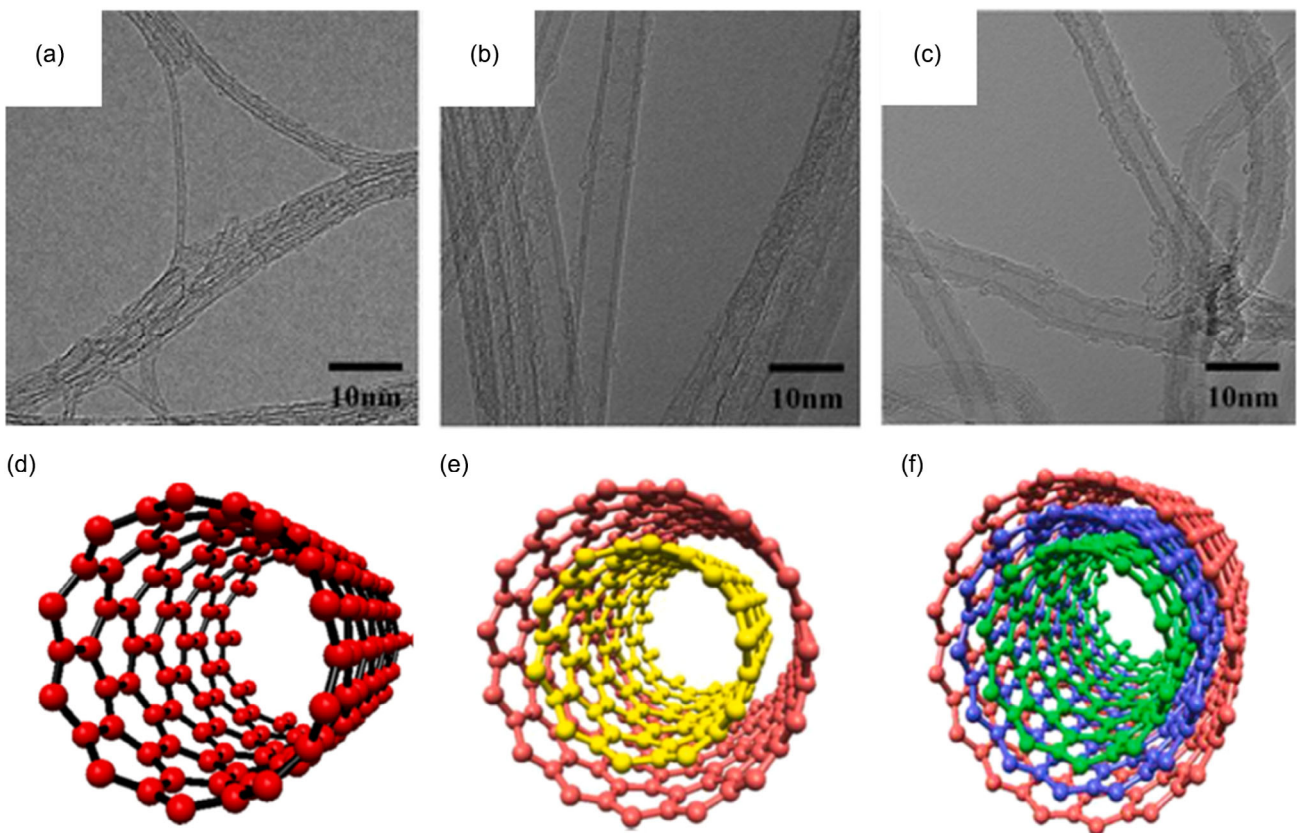


Figure 2. HRTEM images of a) SWCNTs, b) few-walled CNTs, and c) MWCNTs. Reproduced with permission.^[46] Copyright 2009, American Chemical Society. Schematic figures of d) SWCNT, e) DWCNT, and f) MWCNT. Reproduced with permission.^[47] Copyright 2021, Elsevier.

Table 1. Comparison of electrical and mechanical properties and price of SWCNTs, DWCNTs, and MWCNTs. Noteworthy values are highlighted with bold red text.

Properties	SWCNTs	DWCNTs	MWCNTs	References
Diameter [nm]	0.81–2.03	Inner 0.8–2.8 Outer 1.55–15	Inner 3–70 Outer 2–15	[56–59]
Average length [μm]	4–20	≈50	10–30	[60]
SSA [$\text{m}^2 \text{ g}^{-1}$]	400–1000	350	>500	[60]
Tensile strength [GPa]	20.0–24.4	51–84	54.6–148.4	[61–63]
Young's modulus [TPa]	1.2–2.8	0.73–1.33	0.27–0.95	[64–66]
Thermal conductivity [$\text{W m}^{-1} \text{ K}^{-1}$]	3000	≈	10–1000	[67,68]
Resistivity [$\Omega \text{ cm}$]	9.0×10^{-5}	1.0×10^{-6}	$4.4\text{--}12.6 \times 10^{-4}$	[69–71]
The price per gram	\$650	\$364	\$117	[60]

statistics to estimate the tensile strength range of MWCNTs to be between 54.6 and 148.4 GPa. Hsieh et al.^[64] used an elastic model to obtain a Young's modulus of SWCNT ranging from 1.2 to 2.8 TPa. However, the Young's moduli of DWCNT and MWCNT were calculated to be between 0.73–1.33 TPa^[65] and 0.27–0.95 TPa, respectively.^[66]

Wang et al.^[67] devised a modified wavevector model based on the lengths of SWCNTs to obtain an approximate thermal conductivity of $3000 \text{ W m}^{-1} \text{ K}^{-1}$. Based on the thermal boundary

resistance, Prasher^[68] estimated the thermal conductivity of MWCNTs to be $10\text{--}1000 \text{ W m}^{-1} \text{ K}^{-1}$. Many studies on the relationship between electrical resistivity and temperature found resistivities of CNTs at room temperature to, respectively, be 9.0×10^{-5} , 1.0×10^{-6} , and $4.4\text{--}12.6 \times 10^{-4} \Omega \text{ cm}$ for SWCNTs, DWCNTs, and MWCNTs.^[69–71] The prices of SWCNTs, DWCNTs, and MWCNTs from Ossila are \$650.00, \$364.00, and \$117.00, respectively, wherein their prices are based on the difficulty of synthesis.^[60] In the context of energy

device applications, electrical resistance is a critical factor to consider. As observed in Table 1, it is evident that electrical resistance increases as one progresses from SWCNTs to MWCNTs. Moreover, there is a notable trend in cost reduction as the wall count of CNTs increases, making MWCNTs a cost-effective choice.

The hydrophobic surfaces of CNTs make dispersion in water impractical. Thus, it is necessary to modify the chemical properties or use a surfactant in water.^[72,73] One report showed the solubility data of crude CNTs with estimated absorbances using UV-vis absorption spectra.^[74] The “good” soluble solvents enabled absorbances of black and translucent parts of CNT mixtures to be around 0.300. The absorbance of the “excellent” CNT solution is almost 1.000, and a “poor” solvent was defined by CNT precipitation in a visually transparent solution. Table 2 summarizes the solubility of some solvents. Examining the dispersibility of CNTs in various solvents in Table 2, it becomes evident that *m*-dichlorobenzene demonstrates excellent dispersibility for all three CNT types. However, when chlorobenzene is used as the solvent, it is reported that only SWCNTs and DWCNTs exhibit good dispersibility. In contrast, *N*-methyl-2-pyrrolidone (NMP) and dimethylformamide (DMF) solvents exclusively showcase excellent dispersibility for MWCNTs.

Measuring and evaluating the dispersibility of CNTs can be a challenging task. Therefore, in the literature, the evaluation of dispersibility is often conducted using the Hansen solubility parameters (HSPs) that are obtained by assessing the compatibility of solvents with CNTs through these parameters.^[74] We base our understanding of dispersibility on the HSPs.

For SWNTs, a significant proportion of the solvents examined in this study exhibit good solvency characteristics. Consequently, the solubility sphere for SWNTs displays a notably large R_o , consistent with previous findings. However, it should be noted that this behavior is not observed in the case of other CNTs. This discrepancy is likely attributed to the presence of various factors on the surface of SWNTs, such as defects, carbonaceous compounds, and encapsulated catalysts. These heterogeneities, especially the carbonaceous compounds, may possess significantly different HSPs that promote dispersion in a broader range of solvents.

In the case of DWNTs, it is notable that the solubility region appears notably diminished, reflecting the enhanced surface homogeneity within these CNT samples. Regardless of its proximity to the solubility region, acetophenone consistently demonstrates poor solvent characteristics. Conversely,

Table 2. Comparison of SWCNT, DWCNT, and MWCNT dispersibility in several solvents.^[74]

Dispersibility	SWCNT	DWCNT	MWCNT
Toluene	Poor	Poor	Poor
Chlorobenzene	Excellent	Good	Poor
<i>m</i> -dichlorobenzene	Excellent	Good	Good
Dichloromethane (MC)	Poor	Poor	Poor
<i>m</i> -xylene	Poor	Poor	Poor
NMP	Poor	Poor	Good
DMF	Poor	Poor	Excellent

hexachloroacetone and dibenzylether exhibit effective solvent properties, irrespective of their actual HSP parameters.

MWNTs exhibit a unique solubility behavior characterized by a peculiar feature. Interestingly, there are not one but two distinct solubility regions. The first region encompasses the typical solvents for CNTs, while the second one comprises solvents with stronger polar and hydrogen bond contributions. Consistent with the cases discussed earlier, it is anticipated that the MWNT samples consist of structurally and chemically heterogeneous nanotubes. This anomaly is akin to what is observed in the case of thin MWNTs, particularly poor solubility in acetophenone. The hypothesis regarding the inhomogeneity of MWNTs is substantiated by the more regular solubility behavior observed after regraphitization of the nanotubes. The first solubility region exhibits a reduced diameter, and the second solubility group, characterized by high polar and hydrogen bond components, nearly vanishes.

In summary, from the perspective of HSPs, SWNTs, DWNTs, and MWNTs exhibit variations in their solubility parameters and the size of their solubility regions. Consequently, this leads to differences in dispersibility in various solvents.

Graphene is another material aside from CNTs with the potential to be utilized in next-generation energy devices. Researchers have demonstrated that graphene ink serves under specific conditions as an electrocatalyst in experimental dye-sensitized solar cells (DSCs).^[75] However, a serious drawback is poor adherence to the DSC electrodes. Therefore, one important condition to produce the ink is the sufficient dispersion of sodium carboxymethyl cellulose as a binder in a solution of graphene nanoplatelet powder and isopropanol alcohol. An ultrasonic homogenizer is used to achieve the dispersion. The resulting ink is then printed as a catalyst onto a flexible DSC with a reported conversion efficiency greater than 6% at a maximum voltage of 0.68 V. While such results are promising, a major bottleneck to scalable manufacturing of graphene nanoplatelet powder is the lack of sustainable, low-cost graphene production.^[76] There are three essential factors that determine this production: graphite quality, graphene exfoliation efficiency, and graphene dispersibility in a solvent. One method for achieving exfoliation and dispersibility is to use low-boiling-point solvents, such as isopropanol or chloroform, so that greater than 75% of the graphene is dispersed indefinitely.^[77]

Isopropanol is demonstrated by researchers to be particularly efficient at generating graphene.^[76] It is observed, however, that higher degrees of graphene defects lead to reduced dispersibility. By selecting graphene with a surface energy closer to the atomically perfect 68 mJ m^{-1} , such as GR150, dispersibility in isopropanol is improved. A more common solvent recognized for being the most efficient dispersant of graphene is NMP. As indicated in Table 2, the same solvent is particularly effective at dispersing MWCNTs. On the other hand, NMP has a negative impact on the environment, and thus more eco-friendly alternatives, such as isopropanol, are recommended. If such isopropanol is to be used, consideration should be given to using SWCNT, as opposed to MWCNTs. For example, researchers have found the solvent to be useful in dispersing SnO_2 quantum dot-modified SWCNTs to form perovskite/CNT: SnO_2 heterojunctions in the electron transport layers of perovskite solar cells.^[78]

The enhanced transport produces a reported power conversion efficiency from 20.10% to 22.25%.

Yet another alternative to CNTs is MXene with potential energy device applications such as photovoltaics. As with graphene, 2D structures of MXene are desirable because of high transmittance and metallic conductivity. Another similarity to graphene as well as SnO_2 QD-modified SWCNTs is the identification NMP as one of the most effective dispersants.^[79] As an eco-friendlier alternative, isopropanol is a successful dispersant of 2D Ti_3C_2 -MXene in the fabrication of interface layers for CsPbBr_3 solar cells with a 9.01% power conversion efficiency.^[80]

Ultimately, in the development of energy devices, there are multiple factors that potentially determine the selection of CNTs or material alternatives based on architecture. Some include dispersibility, sustainability, and scalability. As discussed in this section, the optimization of dispersibility by selecting a solvent to suite the material architecture could lead to compromised combination of sustainability or scalability. Despite this challenge, there is a growing body of research to guide material selection to optimize target factors.

2.2. Synthesis Methods of CNTs

To access high-quality CNTs at high yields, methods involving arc discharge (Figure 3a), laser ablation (Figure 3b), chemical vapor deposition (CVD) (Figure 3c), and high-pressure carbon monoxide (HIPco) have been deployed by researchers (Figure 3d).^[81,82]

2.2.1. Arc Discharge

The first CNTs were synthesized by arc discharge.^[5] This method is widely used because it does not require expensive equipment such as lasers and complex setup, in contrast to other synthesis methods. Arc discharge utilizes a cathode and anode, generally

composed of graphite and installed in parallel inside a chamber with precursors and catalysts attached to the anode (Figure 3a). Applying a minimum predetermined voltage to the cathode induces current flow, thereby increasing the temperature in the chamber to between ≈ 4000 and 6000 K. At such temperatures, gas is converted into a plasma state that emits ions and electrons. The highly mobile electrons collide with the precursors and catalysts, and carbon ions bond with the cathode and develop into CNTs. The plasma density changes when the gap between the cathode and anode is controlled. Researchers have tuned the properties of CNTs by changing variables such as catalysts, voltage, current, pressure, and gas.^[83–88] Recent discoveries related to applying a magnetic field in the axial or transverse direction to the electrodes during synthesis have enabled researchers to increase the growth rate and enhance the physical performance of such CNTs.^[89–93]

2.2.2. Laser Ablation

Developed by Guo et al.,^[94,95] a laser ablation method comprising the placement of a graphite target at the center of a chamber and the emission of a laser on the target while the surrounding inert gas flows at constant pressure enabled the production of SWCNTs. Consequently, CNTs are deposited on a cooler collector.^[96] This method is significantly more expensive than other methods, owing to the use of lasers. Therefore, they are unsuitable for small-scale laboratories. Several factors influence laser ablation, including the types of gases and lasers, pressure, and catalysts. Some studies have reported the synthesis of SWCNTs and MWCNTs via laser ablation.^[97–102] DWCNTs are typically produced by arc discharge, CVD, and peapod methods.^[103] In a recent study, laser ablation was used to synthesize MWCNTs without catalysts in water for use in MWCNT/Si photodetectors.^[104]

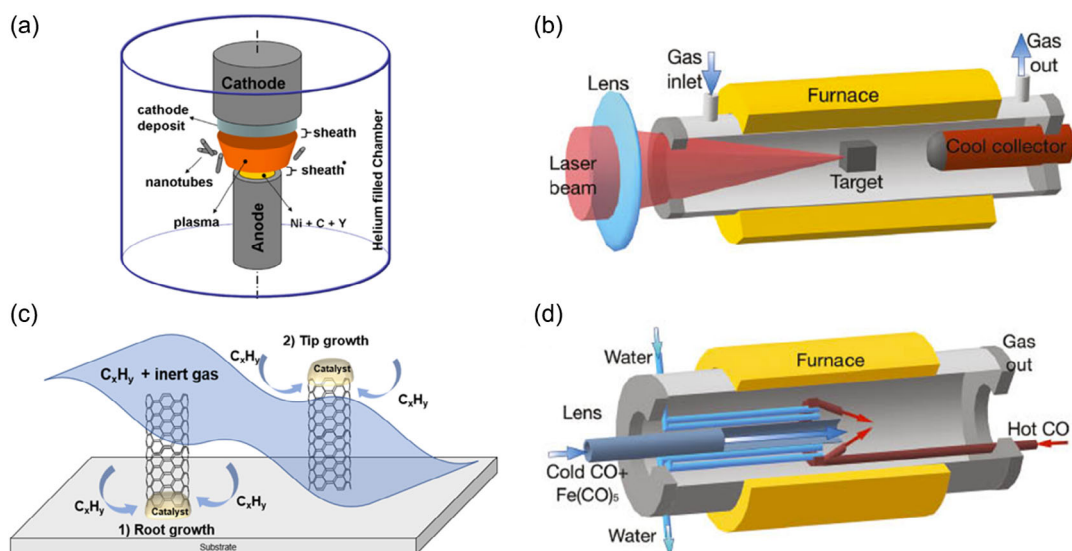


Figure 3. Schematic diagrams of CNT synthesis methods: a) arc discharge. Reproduced with permission.^[82] Copyright 2012, IOP Publishing. b) Laser ablation. Reproduced with permission.^[81] Copyright 2016, De Gruyter. c) CVD and d) HIPco. Reproduced with permission.^[81] Copyright 2016, De Gruyter.

2.2.3. CVD

The most significant disadvantage of the arc-discharge method and laser ablation is the inability to produce CNTs rapidly and in high quantities. Consequently, an alternative method to produce CNTs at scale is needed. CVD has been explored to meet this demand as a cost-effective alternative to producing high quantities of CNTs.

The CVD process involves a metal substrate at a high temperature (typically 600–1200 °C), wherein hydrocarbon precursors (such as methane, acetylene, and benzene) and carbon oxides (such as CO and CO₂) are injected onto the substrate together with inert gases (such as Ar, H₂, N₂, and NH₃). Metal catalysts for this process are usually Fe, Co, Ni, or ferrocene. SWCNTs or MWCNTs can be synthesized by changing specific metal catalysts and other synthesis conditions, such as pressure. CNT growth by reacting precursors fixed on the substrate without catalysts is called “tip growth.” In contrast, “root growth” describes mechanisms involving catalysts that stick to a metal substrate and hydrocarbon bonding that develops CNTs above catalysts.^[47,105,106]

CNT defects often plague CVD technology compared to other synthetic approaches. Recent studies have compensated for this proposal by changing the process method using new catalysts or by adding extra chemicals.^[107–111] Lee et al.^[107] devised a deep-injection floating-catalyst CVD (FCCVD) technique, in which a catalyst containing appropriately bound ferrocene and thiophene was placed in a long and hollow aluminum tube along with all necessary reactants. Methane was the carbon source and was injected with Ar and H₂ gas. This novel synthesis method increased the aspect ratio, crystallinity, and production rate to high levels, demonstrating the possibility of mass production for industrial applications. Ferrocene-derived catalysts employed by this method bonded with oxygen-containing functional groups to improve the SWCNT purity from 79% to 90%. The crystallinity increased approximately fivefold, whereas the I_G/I_D ratio decreased from 74 to 18, thereby improving the physical properties of the CNTs.^[109] Another study designed a high-purity SWCNT synthesis method using the FCCVD method by adding an Ar carrier gas. The injection of Ar gas produced CNTs with a relatively small diameter and even distribution, resulting in enhanced physical stability. This increased physical stability may be attributed to the injection of Ar gas that reduced the reactive radical concentration, thereby causing an etching effect and

enhancing the reactive hydrocarbon species that stably synthesizes CNT.^[110]

2.2.4. HIPco

HIPco is an innovative SWCNT synthesis process designed by a research team at Rice University in 1999.^[112] CO and iron pentacarbonyl (Fe(CO)₅) were mixed and sprayed into a pipe in a high-temperature chamber (800–1200 °C). Then, ion particles triggered the synthesis of SWCNTs according to the following chemical reaction equation:



During CNT synthesis, water coolant flowed into the chamber to maintain a low environmental temperature until immediately before the mixed gas synthesis. Then, the furnace was heated to a high temperature just before the CNT growth reaction. Therefore, it is necessary to regulate the gas mixture's temperature and maintain the gas feed's speed to achieve SWCNT nucleation. Although alternative methods are challenging to scale up owing to variable conditions and high production costs, the HIPco process enables mass-produced SWCNTs with fewer defects and high purity. Consequently, SWCNTs have become more accessible. Drawing from the above discussion,^[47,113,114] Table 3 compares the four mainstream syntheses across several key factors.

3. Enhancing Dispersibility of CNTs

It is commonly understood that hollow p_z orbitals on CNT surfaces induce $\pi-\pi$ attractions among CNTs. This interaction and van der Waals interactions promote aggregation and precipitation, as shown in Figure 4a.^[115] CNTs cannot be dispersed in water or aqueous solutions because of their hydrophobic surfaces. Table 4 provides further details about the dispersion by summarizing the HSPs (δ_D , δ_P , and δ_H) and the maximum dispersibility (C_{Max}) of different solvents, as described in ref.[116] Considering the HSP of CNTs and the revised solubility parameters, good solvents for dispersing CNTs were predicted. N-cyclohexyl-2-pyrrolidone (CHP), NMP, and DMF showed excellent CNT dispersibility, although some refinement is needed to ensure the fit of the parameters to the empirical data.

Table 3. Summary of four kinds of common CNT synthesis methods.

CNT synthesis methods	Arc discharge	Laser ablation	CVD	HIPco
Carbon source	Graphite	Graphite	Hydrocarbon (C _x H _y)	Carbon monoxide (CO)
Product	All	SWCNT or MWCNT	All	SWCNT
Production rate	Low	Low	High	Very high
Per unit cost	High	High	Low	Low
Advantage	High quality Simple process	High quality	Mass production	Mass production
Disadvantage	Purification required Not suitable for small laboratories	High energy requirement	Many defects in product	None

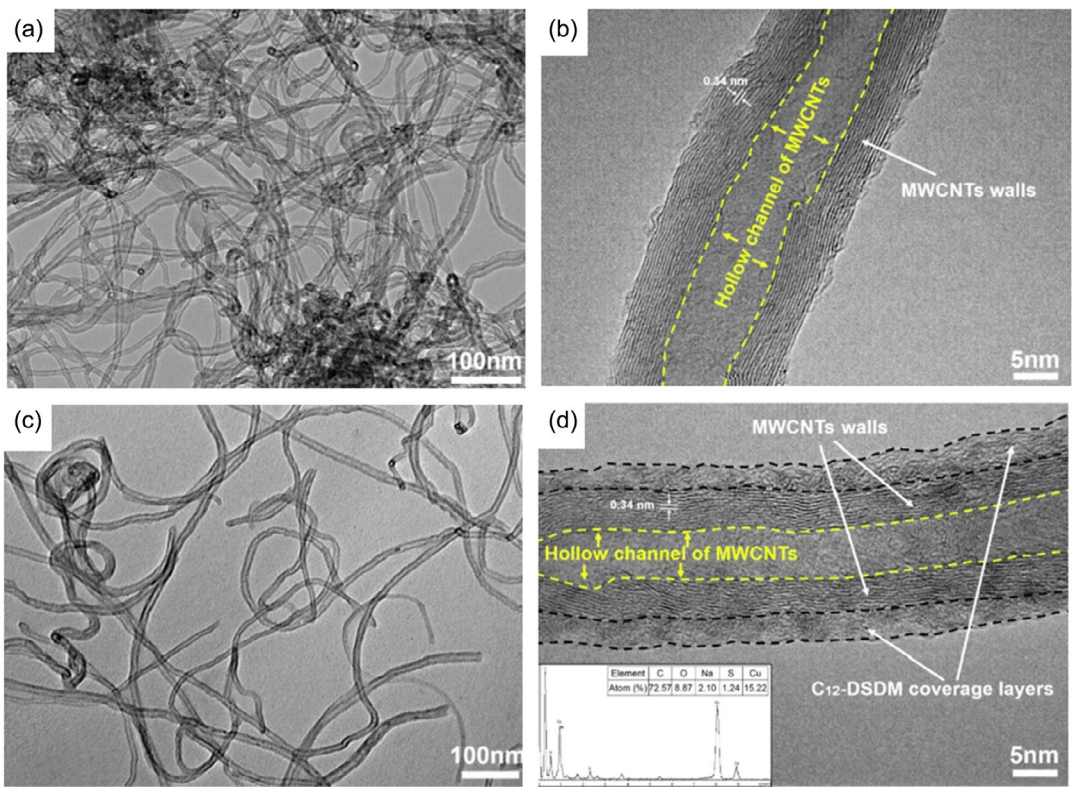


Figure 4. a,b) TEM images of pristine MWCNTs and c,d) C₁₂-DSDM-modified MWCNTs. By comparing (a) and (c), C₁₂-DSDM-modified MWCNTs dispersed better than pristine MWCNTs. C₁₂-DSDM coverage layers on MWCNTs were confirmed by image comparison between (d) and (b). Reproduced with permission.^[115] Copyright 2019, Elsevier.

Table 4. Summary of HSPs (δ_D , δ_p , and δ_H) and maximum dispersibility (C_{Max}) for several solvents. Reproduced with permission.^[116] Copyright 2009, American Chemical Society.

Solvent	δ_D [MPa ^{1/2}]	δ_p [MPa ^{1/2}]	δ_H [MPa ^{1/2}]	C_{Max} [mg mL ⁻¹]
CHP	18.2	6.8	6.5	3.5
NMP	18.0	12.3	7.2	0.116
DMF	17.4	13.7	11.3	0.023
Acetone	15.5	10.4	7.0	0.011
Isopropyl alcohol (IPA)	15.8	6.1	16.4	0.0105
Toluene	18.0	1.4	2.0	0.005
THF	16.8	5.7	8	0
1,1-dichloroethane	16.5	7.8	3	0
MC	18.2	6.1	18.2	0

3.1. Dispersibility Enhancement by Mechanical Processes

Several mechanical dispersion methods can be used to address aggregation: 1) Ultrasonication is used to distribute the CNTs in the solvents finely. Sometimes, other dispersion methods are used in conjunction with ultrasonication to prevent instantaneous reaggregation. The stronger the ultrasonication, the more effective is its ability to disperse CNTs in solvents. However, excess ultrasonication generates defects by damaging CNTs.

2) The ball milling process combined with chemical addition stifles attraction between CNTs.^[117,118] 3) Extrusion techniques form CNT matrix composites that suppress aggregation of CNTs in some cases.^[119,120] 4) Calendering processes produce unaggregated CNTs for flexible CNT electrodes or epoxy matrices.^[121,122]

Ultrasonication, as the most fundamental method, is frequently employed by many researchers, not only for CNTs but also for dispersing various other materials. However, it is worth noting that extended ultrasonication may lead to CNT breakage and a rise in temperature, potentially causing deviations from the desired properties. Ball milling, on the other hand, is utilized not only for dispersion but also for synthesizing functionalized CNTs by introducing various chemical compounds. In contrast, extrusion and calendering processes are methods used to uniformly disperse CNTs within matrices. While extrusion involves compression-based processing, calendering utilizes multiple rollers to achieve a flat CNT matrix. Therefore, in order to achieve CNT dispersion in desired solvents without causing damage, the development and utilization of new dispersants are imperative.

3.2. Dispersibility Enhancement by Chemical Modification of CNTs

Enhancement of dispersibility by chemical modification of CNTs involves understanding the surface chemistry of CNTs; the

reader is encouraged to refer to the cited reviews for a more detailed account of the chemical functionalization of CNTs.^[123,124] It is worth mentioning that the conjugated sp^2 carbon scaffolding, $\pi-\pi$ interactions, and van der Waals forces among CNTs are chemically suppressed to enhance dispersion, in contrast to mechanical dispersion. Chemical modifications of CNTs can be divided into two approaches: covalent and noncovalent functionalization.

3.2.1. Covalent Functionalization Using Defects and Sidewalls

Covalent functionalization involves the covalent bonding of functional groups with a certain degree of hydrophilicity to the CNT surface through a chemical reaction to increase dispersion. This approach is further classified into two subcategories: defects and sidewall functionalization. Defect functionalization involves bonding specific chemicals to the defect sites of CNTs. In contrast, sidewall functionalization involves bonding specific chemicals to CNTs by breaking double bonds to change the hybridized orbitals from sp^2 to sp^3 .^[123]

Defect Functionalization: An oxidative procedure can attach carboxylic groups and other oxygen-bearing functionalities, such as hydroxy, carbonyl, and ester groups, to defect sites on CNTs. This is the stepping stone to replacing oxygenated sites with the desired chemicals. Huang et al. functionalized CNTs with bovine serum albumin proteins via diimide-active amidation.^[125] Several studies have reported the combination of thiolated CNTs with metal substrates or nanoparticles.^[126,127] Similarly, the insertion of silanized CNTs into polymer matrix composites has been reported to increase the dispersibility of MWCNTs in ethanol.^[128]

Sidewall Functionalization: Various types of sidewall functionalization depend on the choice of chemicals, as indicated in Figure 5. Halogens can be attached to CNTs by chemically reacting with the C=C bonds. For example, fluorination can occur in CNTs by inserting gaseous F₂ at 200 °C as a mixture of BrF₃ and Br₂ at room temperature. Combining this process with CF₄ radio-frequency plasma functionalization significantly improves the dispersion relative to unmodified CNTs and substantially alters the chemical characteristics of CNTs.^[129–131] One application of this approach is the development of high-performance gas sensors.^[132] Similarly, chlorinated DWCNTs are used as humidity sensors with considerable dispersion that are repeatable under humid conditions.^[133] Several attempts have been made using Br^[134–136] and hydrogenate^[137–139] CNTs for the same purpose.

3.2.2. Noncovalent Functionalization

Noncovalent functionalization differs from covalent functionalization in maintaining the intrinsic electrical properties of CNTs. This is because the functional groups that improve the dispersibility bind to CNTs indirectly without breaking the double bonds. Noncovalent functionalization is primarily divided into endohedral and exohedral techniques. Endohedral functionalization injects chemicals inside CNTs through capillary action. For example, there were some reports that fullerenes and alkyl chains were inserted into CNTs.^[140]

However, exohedral functionalization relies on amphiphilic chemicals that induce hydrophobic–hydrophobic interactions with the CNT surfaces on one end. In contrast, the opposite end of the molecule causes hydrophilic or hydrophobic interactions depending on the choice of solvent. These molecules are known as dispersants, surfactants, or binders. Owing to this process's simplicity and inert nature, exohedral functionalization has been particularly favored by researchers in the industry. The structure of the dispersants varies depending on the solvent in which we are dispersed and the target application. One of the few disadvantages of this approach is that the addition of dispersants produces CNTs with a higher overall weight and potentially lowers the conductivity. Therefore, it is crucial to optimize the structural design of surfactants to address this issue, as detailed in Section 3.3.

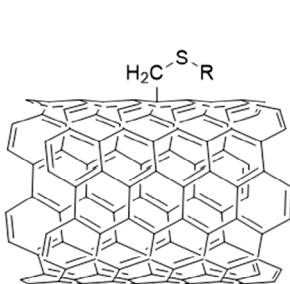
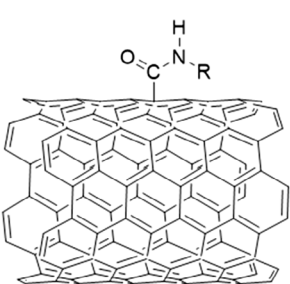
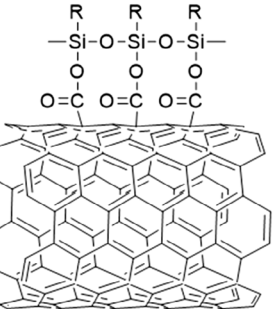
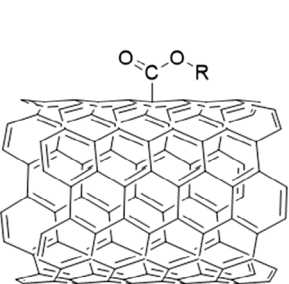
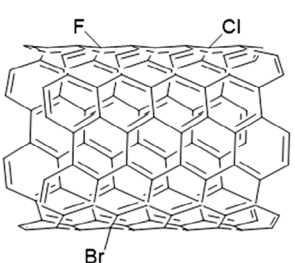
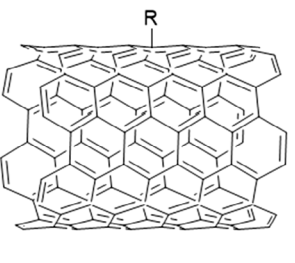
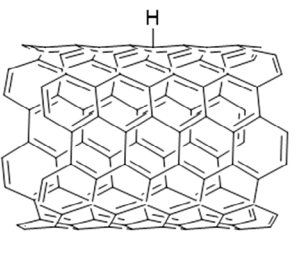
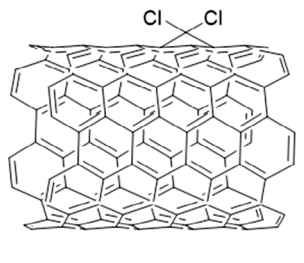
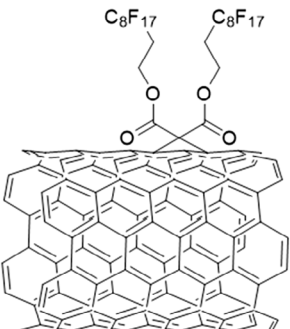
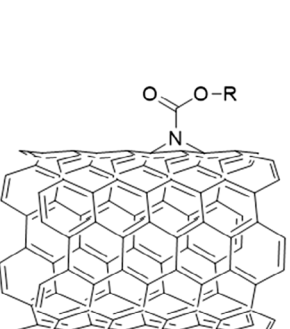
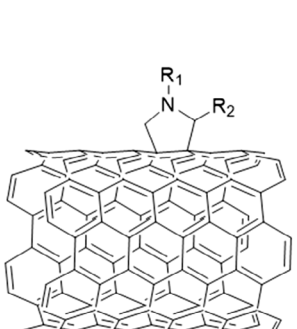
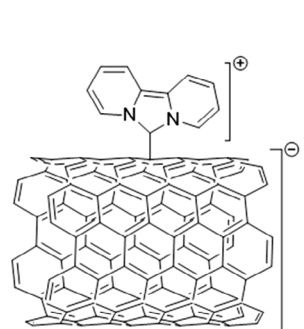
3.3. Noncovalent Functionalization of Dispersants

3.3.1. Amphiphilic Dispersion of CNTs in Water and Aqueous Solutions

Water is an eco-friendly and versatile solvent used in various applications, to which CNTs contribute significantly. However, the intrinsic hydrophobicity of pristine CNTs inhibits their dispersion in aqueous solutions. The application of dispersants composed of a hydrophobic part on one end to interact with CNT surfaces and a hydrophilic part on the opposite end to interact with a polar solvent promotes dispersion in aqueous solutions.

Single-Tail Surfactants: Single-tail surfactants composed of a hydrophilic head and hydrophobic tail disperse the CNTs in water and aqueous solutions. Sodium dodecyl sulfate (SDS),^[141] sodium dodecylbenzenesulfonate (SDBS),^[142] cetyltrimethylammonium bromide (CTAB),^[143] and Triton X-100^[144] are some commonly used surfactants, among which SDBS is the most effective at dispersing MWCNTs and SWCNTs. Although the dispersing capacity has been reported as SDBS > CTAB ≈ cetylpyridinium chloride > sodium tetradecyl sulfate > tetradecyltrimethylammonium bromide (TTAB) ≈ SDS > dodecyltrimethylammonium bromide (DTAB),^[145] many researchers have attempted to develop a novel surfactant to enhance CNT dispersibility.

Recently, Xin et al. synthesized four silicone-based surfactants, S1E19, S2E38, S2E16, and S1E16P8, considering that CNTs interact strongly with siloxane groups. S1E16P8 showed the greatest dispersibility with a CNT concentration of 0.059 mg mL⁻¹, associated with introducing 1 mg mL⁻¹ of the dispersing agent.^[146] Bass et al. combined a poly(styrene) block that induced $\pi-\pi$ stacking with CNTs and a hydrophilic poly(acrylic acid) block to improve the dispersion stability. They determined that styrene in the polymer backbone makes a $\pi-\pi$ stacking on CNT surfaces using optical probes (Rhodamine 6G and Reichardt's dye).^[147] Mohamed et al. measured the electrical conductivity of a nanocomposite using the novel surfactant sodium 1,5-dioxo-1,5-bis(3-phenylpropoxy)-3-((3-phenylpropoxy) carbonyl) pentane-2-sulfonate (TCPH). The three phenyl groups in this surfactant were attached to the CNT surfaces via $\pi-\pi$ interactions. Therefore, TCPH improved the stability of the MWCNT

Defect functionalization

Thiolation

Amidation

Silanization

Esterification
Sidewall functionalization

Halogenation

Radical Addition

Hydrogenation

Carbene

Nucleophilic Cyclopropanation

Nitrenes

Azomethine Ylides

Nucleophilic Carbenes
Figure 5. Examples of defect and sidewall functionalization.

colloid mixture in natural rubber latex, showing better dispersibility than the SDBS surfactant.^[148] Another single-tail surfactant, alkylphenol polyoxyethylene ether (APEO), also has benzene rings that favor the CNT surfaces and hydrophilic chains. The best dispersibility ratios for MWCNTs-OH and APEO were 0.2:1.^[149] An anionic star-like surfactant comprises a hydrophobic polypropylene glycol backbone and five hydrophilic anionic chains. The MWCNT/SDBS suspension precipitated after 10 days, although the CNT mixture with the star-like surfactant was well dispersed for more than 30 days.^[150] Li et al. synthesized a safe and inexpensive surfactant (AEP-4) using a phenolic resin. The MWCNT suspension containing AEP-4 demonstrated more excellent dispersion than the MWCNT suspension containing conventional SDBS. AEP-4

contained relatively more abundant benzene rings, which induced greater $\pi-\pi$ stacking with the MWCNT surfaces.^[151]

Gemini Surfactant: The limitation of the surfactants discussed thus far is inadequate adhesion to CNTs arising from having only one head–tail pair (**Figure 6a**). Therefore, the Gemini surfactants^[152] illustrated in Figure 6b were developed to overcome this problem. The two heads, two tails, and spacer of Gemini surfactants possess significantly improved adhesion and interaction with CNTs.

Hou et al. synthesized an ionic Gemini surfactant, 4,4'-di(*n*-tetradecyl) diphenylmethane disulfate salt (DSDM). DSDM has two alkyl chains, and benzene rings firmly anchored to MWCNT surfaces. According to the UV-vis absorption spectra, the DSDM/MWCNT suspension absorbed more light than the

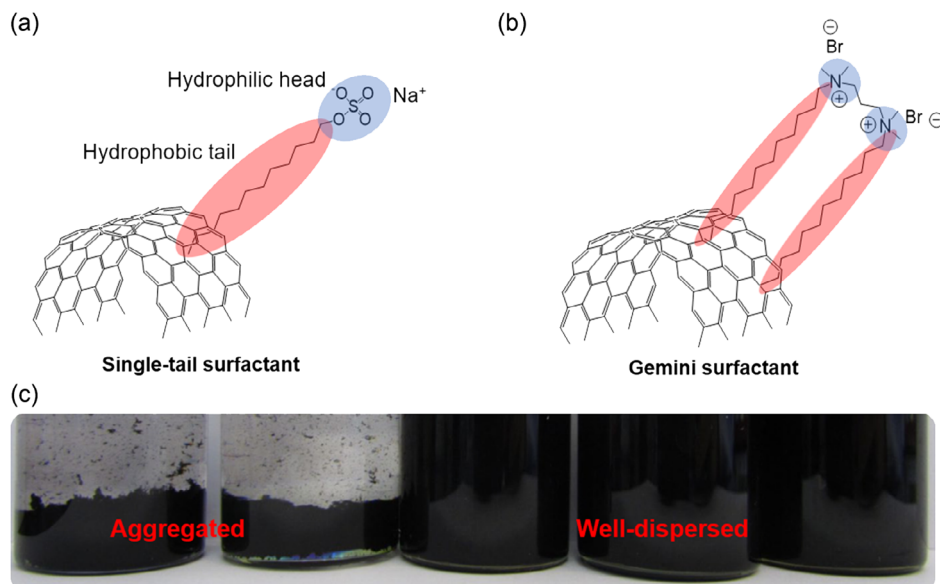


Figure 6. Schematic images of a) single-tail surfactant and b) Gemini surfactant. c) Comparison of aggregated CNTs and well-dispersed CNTs using ST100, ST82, ST58, and ST44 in toluene. Reproduced with permission.^[168] Copyright 2022, Elsevier.

SDBS/MWCNT suspension, indicating the greater dispersibility of DSDM than SDBS in water.^[153] *N,N*-Decyldiquinoliniumdodecylate, another cationic Gemini surfactant, was well dispersed in water based on zeta potential measurements. Applying this surfactant to polyvinyl alcohol (PVA)/CNT nanocomposites resulted in homogeneous dispersion of MWCNT, as measured by Raman spectroscopy, X-ray diffraction, and scanning electron microscope (SEM) analyses. The electrical conductivity of the PVA/CNT nanocomposites was enhanced by increasing the CNT content up to 2 wt%.^[154] Abreu et al. tested the efficiency of several newly synthesized dicationic Gemini surfactants (so-called 12-s-12, 14-s-14, and 16-s-16) against conventional surfactants, such as DTAB, TTAB, and CTAB, in water. Gemini surfactants induced much greater dispersion than single-tailed surfactants. Interestingly, in the case of 12-s-12 and 14-s-14, the maximum concentration of CNTs ($C_{\text{CNT},\text{max}}$) increased with increasing spacer length.^[155]

Biomaterials: CNT dispersants for aqueous solvents generally comprise aromatic compounds or hydrophobic polymer chains on one end and hydrophilic parts on the other. The latter faces away from the CNTs. Biomaterial-based dispersants have the same structure and have been used as CNT dispersants in aqueous solvents. However, biomaterials have eco-friendliness, lower costs, and biodegradability advantages. Unlike artificial dispersants, biomaterial-based dispersants can be obtained from nature and used directly with minor modifications.

Zhang et al. used rosemary acid (RosA) to disperse MWCNTs in dimethyl sulfoxide (DMSO)/H₂O. RosA consists of two benzene rings, forming π - π stacking on the MWCNTs and hydrophilic hydroxyl groups. The prepared composite fibers of PVA/MWCNTs with RosA show remarkable improvements in the tensile strength and Young's modulus tests (Figure 7).^[156] Li et al. compared the solubility of SWCNTs in water using biomaterial-based dispersants composed of peptides, commercial

surfactants, DNA, and water-soluble polymers. The highest dispersibility below the critical micelle concentration (CMC) was obtained for the surfactant based on the peptide aptamer A2. The molecular dynamics demonstrated by the aromatic units in A2 produced a π - π interactions with the SWCNT surfaces.^[157] Zhu et al. applied amphiphilic nanofibrillated cellulose (NFC) to a flexible humidity sensor composed of CNTs. NFC contains many hydroxyl groups that form hydrogen bonds with water molecules. The backbone of NFC was adsorbed onto the CNT surfaces via the hydrophobic–hydrophobic interactions.^[158] Another study by Toshimitsu et al. identified riboflavin (Vitamin B2) as a dispersing agent for SWCNT. Using molecular dynamics calculations, they suggested that there are π - π interactions and hydrogen bonding between riboflavin and SWCNTs.^[159] However, in another study by Chaudhary et al. it was discovered that the protein, α -synuclein, was an effective dispersant for SWCNTs in water. The α -synuclein-dispersed SWCNTs exhibited higher colloidal stability than the Pluronic F127-dispersed SWCNTs concerning UV-vis absorbance at 660 nm for 35 days.^[160] Zhao et al. synthesized a natural α -amino acid derivative, N-dodecanoyl leucinate, for the dispersion of SWCNTs. They suggested that N-dodecanoyl leucinate activated charge transfer to the SWCNTs, resulting in the selective dispersion of semiconducting SWCNTs with a minimal shift in the G⁺ band.^[161] Table 5 shows some recent CNT dispersants used in water and aqueous solvents.

3.3.2. Dispersion of CNTs in Organic Solvents: Steric Stabilization

The CNT dispersants for organic solvents that attach to CNT surfaces are π -conjugated polymers, aromatic materials, and hydrophobic chains. Dispersants for organic solvents rarely contain ionic groups, meaning they do not harness electrical repulsion. Therefore, it is crucial to balance the solvophobic moieties

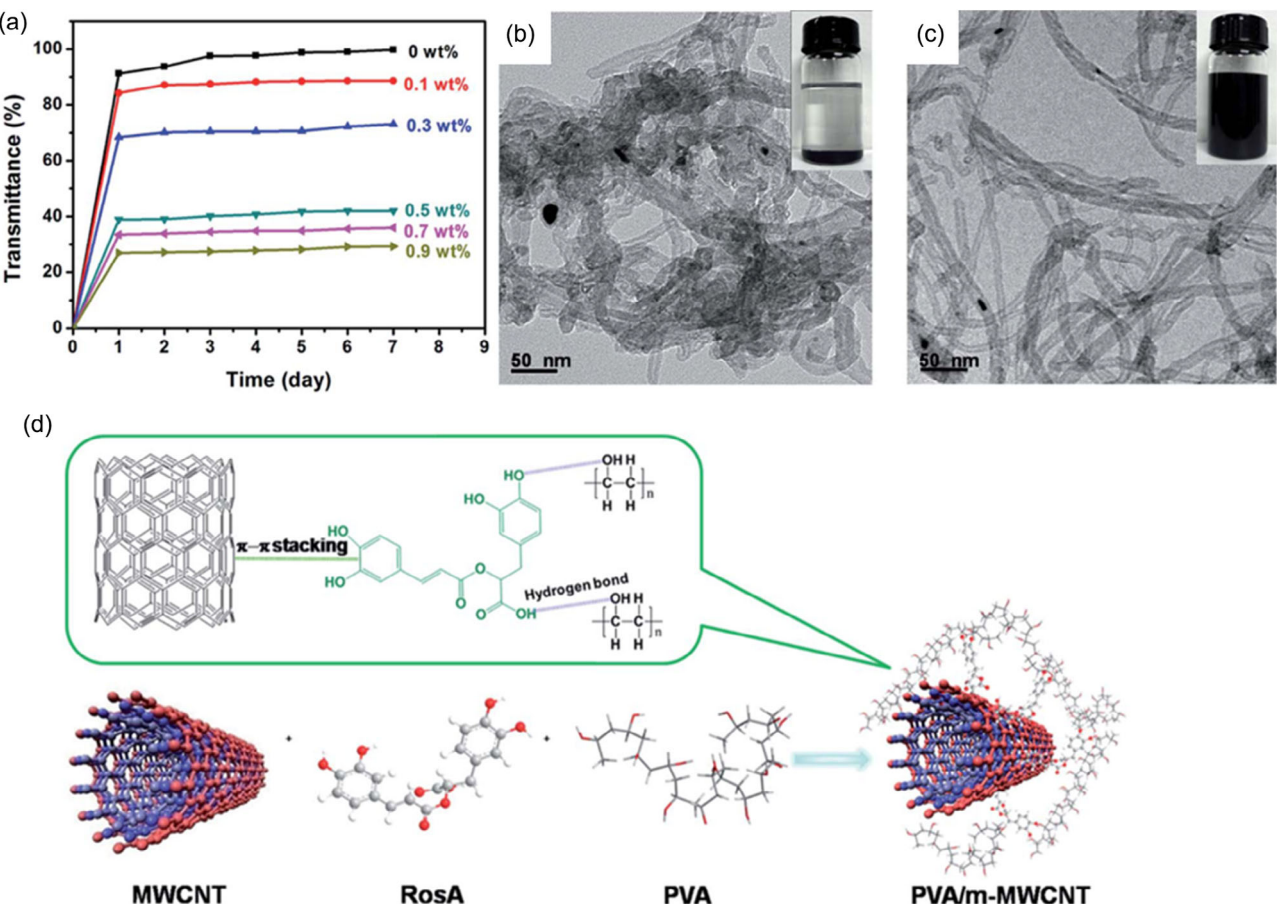


Figure 7. a) UV-vis transmittance of MWCNTs solutions in DMSO H₂O (vol ratio = 3/1) with 0, 0.1, 0.3, 0.5, and 0.9 wt% of each RosA concentration over 7 days. b) TEM images of *p*-MWCNTs. c) TEM images of *m*-MWCNTs. d) Schematic explanation of PVA/*m*-MWCNTs composite structure. Reproduced with permission.^[156] Copyright 2015, RSC Publishing.

by chemically tuning the structures of the dispersants depending on the polarity and structure of the organic solvents.

Lee et al. dispersed SWCNTs with high aspect ratios in tetrahydrofuran (THF) using a dispersant composed of poly((furfuryl methacrylate)-co-(2-(dimethylamino)ethyl methacrylate)) (p(FMA-co-DMAEMA)). They then applied dispersed SWCNTs to a polyethylene substrate to fabricate transparent conductive films (TCFs). Researchers have observed that SWCNT-based TCFs exhibit a remarkable reduction in sheet resistance and high transmittance.^[162] Furthermore, the same authors modified p(FMA-co-DMAEMA) to quaternized p(FMA-co-DMAEMA) (p(FMA-co-QDMAEMA)) through the quaternization of the amine group. They found that p(FMA-co-DMAEMA) was only soluble in THF, and p(FMA-co-QDMAEMA) showed outstanding dispersibility in ethylene glycol (EG), methanol (MeOH), and DMF.^[163] In another study, Zhai et al. used ferrocene to synthesize the dispersant poly(2-(methacryloyloxy)-ethyl ferrocene-carboxylate) (PFcEMA) with an exquisite structure. Ferrocene-induced π - π stacking between cyclopentadiene rings and CNT surfaces. The maximum CNT concentration obtained using PFcEMA was 0.21 mg mL⁻¹ in chloroform.^[164] Park et al. synthesized novel triblock copolymers by combining

three polyimide homopolymers. Among the triblock copolymers, TB1a was the most effective solubilizing agent in THF. The TB1a/epoxy/SWCNT films showed incremental improvements in tensile strength, modulus, and elongation over epoxy without SWCNTs.^[165] Liang et al. used polymers containing carbazole (Car) pendants and hydrophilic PEG to disperse MWCNTs in THF. The investigators were able to maintain the dispersion of the MWCNTs for over 30 days.^[166] 2-N-morpholinoethyl methacrylate (MEMAs) was copolymerized with dodecyl methacrylate and ST. Dispersibility was estimated based on the reactivity ratio. The nucleobase-functionalized poly(acrylamide) polymers were tested for SWCNT dispersion in a mixture of THF and DMF. The thymine-functionalized acrylamide produced the most stable SWCNT dispersion.^[167] The ST/MEMA copolymer containing 42 mol% MEMA (ST58) demonstrated the most effective dispersion among the copolymer alternatives, with the dispersion lasting up to 10 days (Figure 6c).^[168]

Polycyclic aromatic hydrocarbons (PAH) can strongly interact with the π -conjugations on the CNT surfaces. Consequently, many researchers have combined other chemicals with PAH to synthesize CNT dispersants.^[169–172] Wang et al. synthesized pyrene-functionalized polymers (PAEK-Pys) via C–H borylation

Table 5. Review of recent CNT dispersants used in water and aqueous solvents.

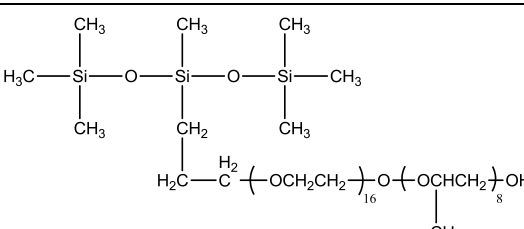
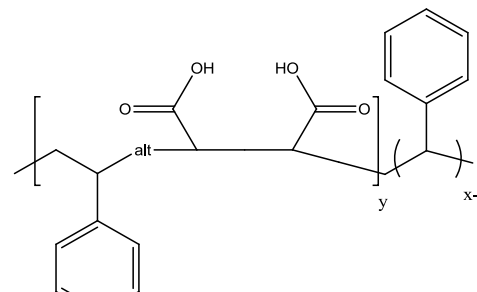
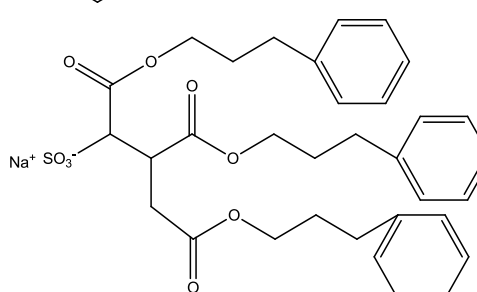
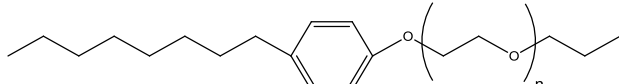
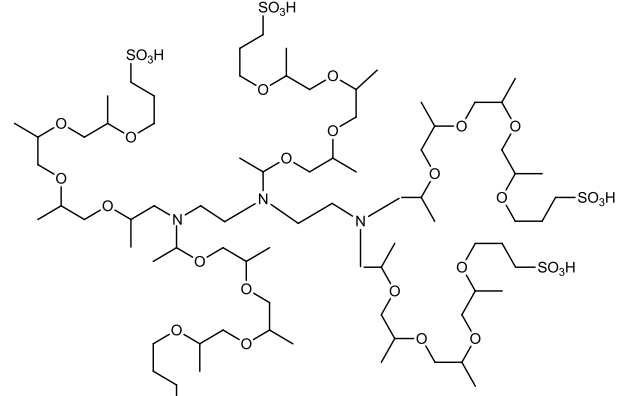
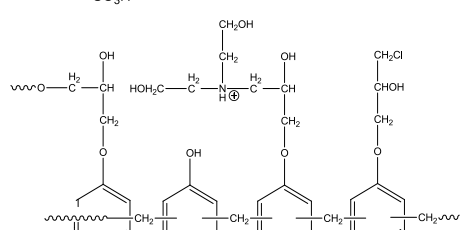
Year ^[Ref.]	Dispersant	Solvent	Features
2015 ^[146]		Water	Silicone surfactant $C_{\text{CNT,mac}} = 0.059 \text{ mg mL}^{-1}$
2015 ^[147]		60:40 DMSO:H ₂ O	Polymeric surfactant
2015 ^[148]		Water	Three phenyl group Applied to NR-latex
2017 ^[149]		DI water	Dispersion MWCNTs-OH
2018 ^[150]		Ultrapure water	Star-like structure Higher storage ability than SDBS
2018 ^[151]		DI water	Better dispersion than SDBS

Table 5. Continued.

Year ^[Ref.]	Dispersant	Solvent	Features
2018 ^[153]		DI water	Anionic Gemini surfactant Better dispersion than SDS Improving mechanical properties of DSDM-CNT/Mg matrix
2019 ^[154]		DI water	Cationic Gemini surfactant Applied in PVA matrix
2019 ^[155]		Ultrapure water	Cationic Gemini surfactant Better dispersion than DTAB, TTAB, and CTAB

and Suzuki coupling reactions. The chloroform concentration of SWCNTs with PAEK-Py-10 was 0.272 mg mL^{-1} , greatly enhancing CNT dispersibility.^[173] Adronov et al. tested the dispersibility of SWCNTs using a strained alkyne-containing polymer backbone with seven cycloadducts. The dispersant containing aromatic compounds and a ketone functional group improved the dispersibility of the SWCNTs in THF.^[174] Polyphenylene sulfones (PPSUs) were synthesized using pyrene monomers to enhance their thermal and mechanical stabilities. The highest MWCNTs concentration in NMP was 0.700 mg mL^{-1} using PPSU with 20% pyrene groups.^[175] **Table 6** summarizes some recent CNT dispersants used in organic solvents.

4. Dispersant-Based CNTs in Energy Device Applications

Due to the limitations of graphite performance, research is actively exploring alternative materials, among which CNTs stand out as highly attractive candidates. CNTs, possessing excellent mechanical and electrical properties, are considered suitable for use in battery electrodes. SWCNTs have a reversible capacity ranging from 300 to 600 mAh g^{-1} , significantly surpassing the capacity of widely used battery electrode material, graphite (320 mAh g^{-1}). Moreover, mechanical and chemical treatments of SWCNTs can further elevate their reversible capacity to as high as 1000 mAh g^{-1} . However, when used as anodes, a major challenge with CNTs is the irreversible lithium-ion capacity. Aggregation of CNTs in the anode leads to increased insertion of lithium ions during the initial charge, leading to irreversible

lithium-ion consumption. Additionally, the aggregation issue contributes to a lack of stable voltage plateaus during battery discharge.^[16]

For supercapacitors, using electrolytes with high operating voltages necessitates electrode materials devoid of oxygen-containing functional groups such as COOH, OH, or C=O. This is because these groups are prone to decomposition at high voltages. In supercapacitors, reducing internal resistance and densification are crucial. Therefore, chemical modifications, particularly the addition of oxygen-containing groups for the dispersion of CNTs, may not be suitable for supercapacitor applications as they can compromise electrical conductivity. Addressing the dispersion issue of CNTs is deemed critical, and our research suggests that developing an appropriate dispersant model is essential for applying CNTs in energy storage devices. The newly developed dispersant should not only ensure dispersion but also guarantee special properties, such as maintaining electrical conductivity when incorporated into battery cathodes or supercapacitors.^[176]

The application of CNTs is one of various research trends in material developments toward the advancement of energy device technologies. Within the scope of energy storage, ruthenium nanoparticles, microporous carbon, carbon/metal composites, and microporous polymers based on double-decker silsesquioxane are merely a few of the materials that have been incorporated into capacitors.^[177–179] Among the abundant selection of candidates for bringing forth the next generation of energy storage devices, exceptional conductivity and 1D morphology make CNTs especially desirable.^[180] As years of research have demonstrated, however, the advantageous properties of CNTs are

Table 6. Overview of recent CNT dispersants used in organic solvents.

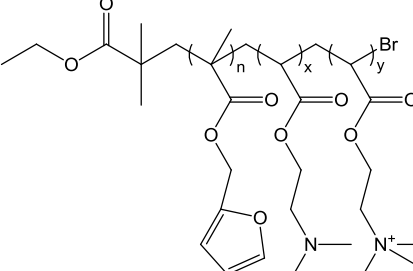
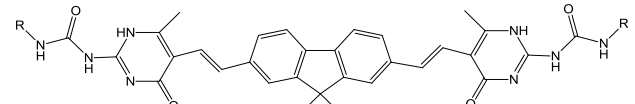
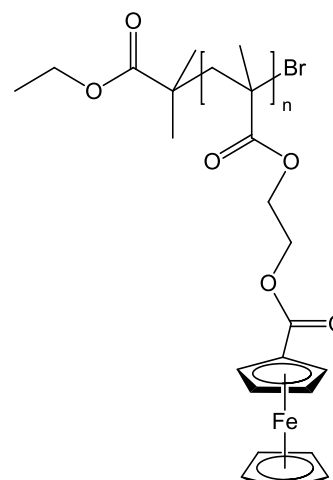
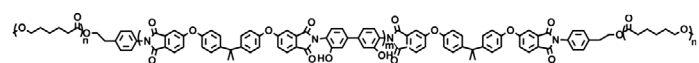
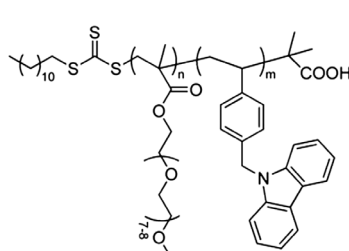
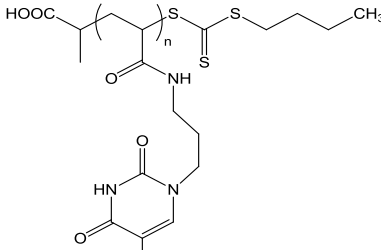
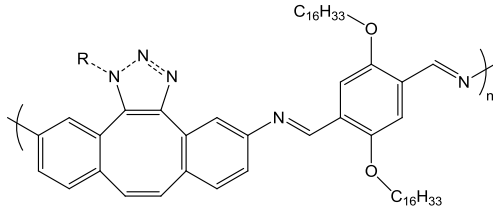
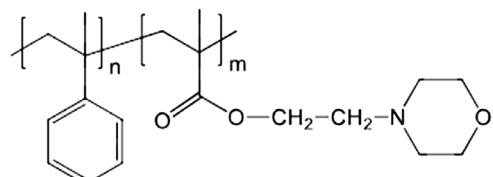
Year ^[Ref.]	Dispersant	Solvent	Features
2015 ^[162]		EG, MeOH, and DMF	Polymeric dispersant
2015 ^[211]		Toluene	Selective semiconducting SWCNTs dispersion
2015 ^[164]		Chloroform	Contains ferrocene
2017 ^[165]		THF	Triblock copolymer Improves mechanical properties of SWCNT/epoxy composites
2017 ^[166]		THF	Contains Car pendants
2017 ^[167]		THF + DMF	Contains synthetic nucleobase
2018 ^[174]		THF	Selective dispersion by changing sidechains

Table 6. Continued.

Year ^[Ref.]	Dispersant	Solvent	Features
2020 ^[175]		NMP, DMF, and Chloroform	Contains pyrene High mechanical and thermal stability
2022 ^[168]		Toluene	Copolymerization

severely offset by limited specific capacitance. Relevant studies thus endeavor to address this major challenge by integrating CNTs as additives into other substances.^[181–183]

The state of innovative materials for electrode fabrication echoes that of capacitors. CNTs are also one of a growing list that includes such widely considered candidates as transition metal oxides in lithium-ion batteries^[184] and highly porous graphitic biomass carbon as a potentially low cost, eco-friendly in supercapacitors.^[185] Hindered by extreme synthesis conditions and complicated fabrication methods, researchers often relegate CNTs to additives in electrode materials.^[180]

Despite the ongoing challenges to the scalable adoption of CNTs in energy devices, there is a subset of studies that convey promising results. To circumvent the decreasing effectiveness of binders between current collectors and active materials over the course of metal ion battery charging cycles, binder-free batteries featuring CNTs that are grown onto the current collectors to interface with the active materials have become an appealing alternative.^[180] However, there is a yet unsolved lack of cohesion among CNT structures with the electrodes.

What follows, therefore, is an overview of other studies that make progress through the dispersion of CNTs as an essential fabrication step while maintaining cohesion. As a way of providing an incisive perspective on these studies, the current survey covers two types of applications: energy storage and energy conversion. Although the dearth of existing literature on CNT dispersion toward the implementation of energy devices prohibits a thorough discussion, the opportunity will be taken to identify energy device applications that warrant further experimental exploration.

With regard to the application of CNTs to battery electrodes, researchers have considered anode films. Cui et al.^[28] increased the thin silicon films that can be used as anodes in lithium-ion batteries using CNT networks. Pure silicon films for anodes have deficient cycling performance owing to structural deformation

when Li ions intercalate and deintercalate. However, the infiltration of CNTs into the Si anode resulted in a higher specific charge storage capacity and improved the cycling effect. Ripples formed on the CNT–Si anodes endured pulverization of Li ions during cycling. The CNT network was formed from the ink containing SDBS surfactants in water.^[28] Liu et al.^[186] compared the electrochemical performance of conductive CNT films composed of SWCNTs (Figure 8c), DWCNT (Figure 8d), and MWCNTs (Figure 8e). Triton X-100 was used to disperse the CNTs in distilled water. MWCNTs showed an inferior specific charge compared with SWCNTs and DWCNTs after the first half-cycle reduction. However, from the fifth cycle onward, the specific charge of the SWCNT and DWCNT films dramatically decreased at 200 mAh g⁻¹, and the MWCNTs maintained 300 mAh g⁻¹. This indicated that MWCNTs were better anodes than SWCNTs and DWCNTs (Figure 8b).^[186] MoS₂ has received considerable attention as an alternative anode material for rechargeable batteries. However, MoS₂ has significant disadvantages, such as swelling during the charge–discharge cycle and poor electrical conductivity. Graphene nanosheets and CNTs were applied to MoS₂ nanocomposites to solve these problems. The CNTs dispersed by SDBS enhanced the electron transport between the graphene and MoS₂ nanocomposites. In addition, the electrochemical performance in rate capability and cyclability improved significantly compared to nanocomposites without CNTs.^[187] Abbas et al. synthesized hexagonal ZnO/CNT nanocomposites to replace graphite anodes. The CNT networks enhanced the capacity and cycle life of the anodes compared with other Zn-based anodes. Self-made CNTs were dispersed using polyvinylpyrrolidone surfactants.^[188]

Injecting CNTs into cathodes has been reported to increase the electrochemical performance and stability of rechargeable lithium-ion batteries.^[189–191] CNTs in the electrospun LiFePO₄/CNT/C composite nanofibers enhanced the cathodes' stability by reducing the nanofibers' carbon defects.

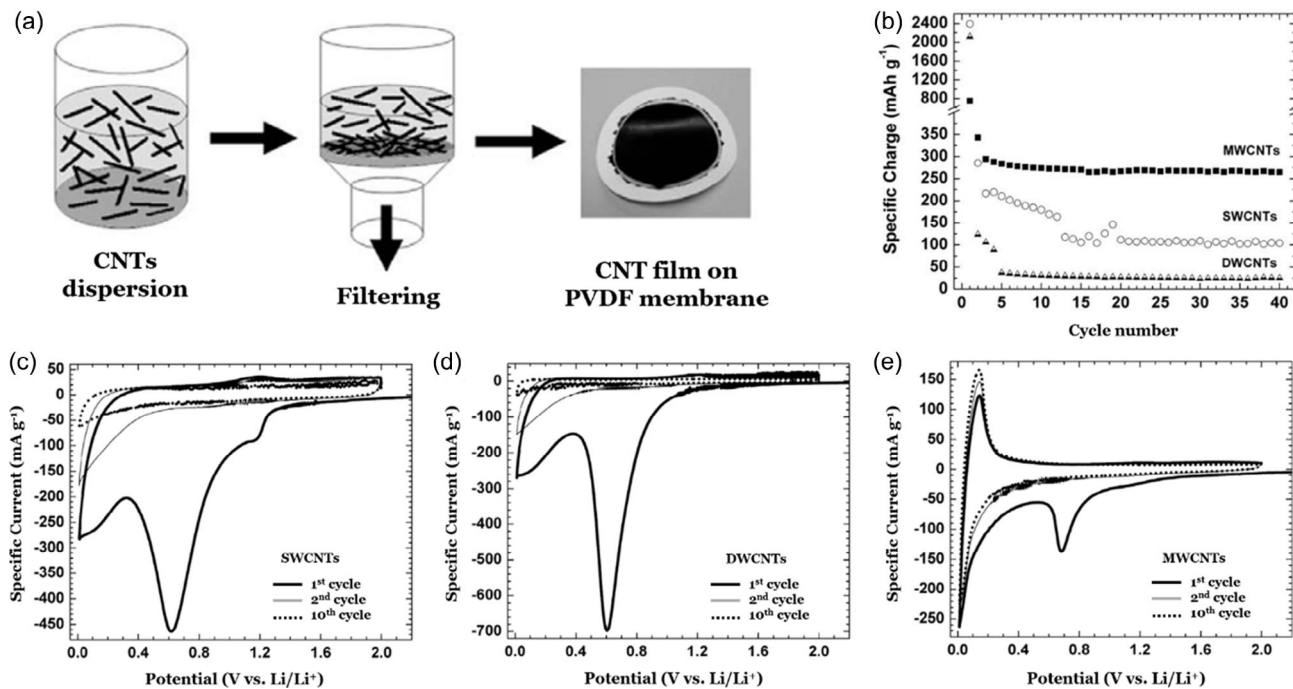


Figure 8. a) Process of preparing CNT films. b) Tendency of specific charges in 40 cycles among three thin film electrodes measured to be 0.01–2.00 V versus Li/Li⁺ at a specific current of 25 mA g⁻¹. Cyclic voltammograms at first, second, and tenth cycle for three thin electrodes for c) SWCNTs, d) DWCNTs, and e) MWCNTs. Reproduced with permission.^[186] Copyright 2009, Elsevier.

The LiFePO₄/CNT/C composite nanofibers showed excellent properties in terms of charge transfer resistance, cycling performance, and rate capabilities compared to pristine LiFePO₄ powders and LiFePO₄/C composite nanofibers. CNTs were functionalized with COOH and mixed with Triton X-100 to enhance dispersibility before being applied to the nanofibers.^[190] Wu et al. introduced CNTs in Li(Ni_xCo_yMn_zO₂) (NCM) cathodes using SDBS to enhance electron transfer and depolarize the electrodes. The NCM523/CNT cathodes improved the cycling and rate performance by 25% compared to NCM523.^[191] Hu et al. enhanced the performance of rechargeable lithium-oxygen batteries (Li–O₂) using a 3D interconnected structure of MoS₂/CNTs nanosheets (Figure 9a). The mesoporous nanostructure increased the contact area between the reaction sites and the electrolyte. In contrast, the CNTs enhanced the electronic conductivity of the cathode. This study used functionalized CNTs with SDBS dispersants to maintain dispersion for an extended period. As a result, the MoS₂/CNTs cathodes showed a high discharge capacity, rate capability, and low overpotential. They increased cycle life compared to other MoS₂ cathodes and super P electrodes (Figure 9b, c, d).^[189]

Covalent organic frameworks (COFs) have become another subject of interest for dispersing CNTs used in energy storage. One study by Samy et al. utilized pyrene to functionalize a framework for improved dispersion.^[192] Blending tetraphenylethylene benzoxazine monomers with SWCNTs produced a composite containing π - π stacks between SWCNT and pyrene units. The composite was subjected to thermal curing to promote SWCNT dispersion. Incorporation of this framework into

a supercapacitor achieved a capacitance of 84 F g⁻¹ at 0.5 mV s⁻¹, along with a stable 98.33% capacitance retention rate for 2000 cycles.

Another study concerned the use of conjugated microporous polymers (CMPs) in combination with SWCNTs.^[193] Using Sonogashira–Hagiura cross-couplings of pyrene, tetrabenzo-naphthalene (TBN) monomers, tetraphenylethylene (TPE), and Car, the researchers produced TBN–TPE–CMPs. By blending these polymers with SWCNTs, a composite with dispersed CNTs was formed with a capacitance retention of 99.18% over 2000 cycles and a capacitance of 430 F g⁻¹ at current density of 0.5 A g⁻¹. There was also a study on 1,3,4-oxadiazole-linked CMPs to increase capacitance to 504 F g⁻¹, although the capacitance was relatively lower at 91.1% per 2000 cycles.^[194]

Whether the topic of interest is capacitive substances or battery electrodes, limited consideration is given to the application of dispersed CNTs. While the studies that are reported cumulatively focus on energy storage, there is a wanting availability of studies on energy conversion. For instance, energy device applications of CNTs include SWCNTs with semiconducting-selective deoxycholate surfactants were added to perovskite solar cells to improve the power conversion efficiency by functioning as a charging bridge between perovskite grains and passivator of interfacial defects.^[55] The efficiency of the solar cells increased from 18.1% to 19.5%. Later, an even more advanced surfactant was synthesized to apply analogue SWCNT to perovskite solar cells.^[195] The newly synthesized 4,6-di(anthracen-9-yl)-1,3-phenylene bis(dimethylcarbamate) (DPB) is composed of a nanotweezer-like anthracene on one end and a stronger-

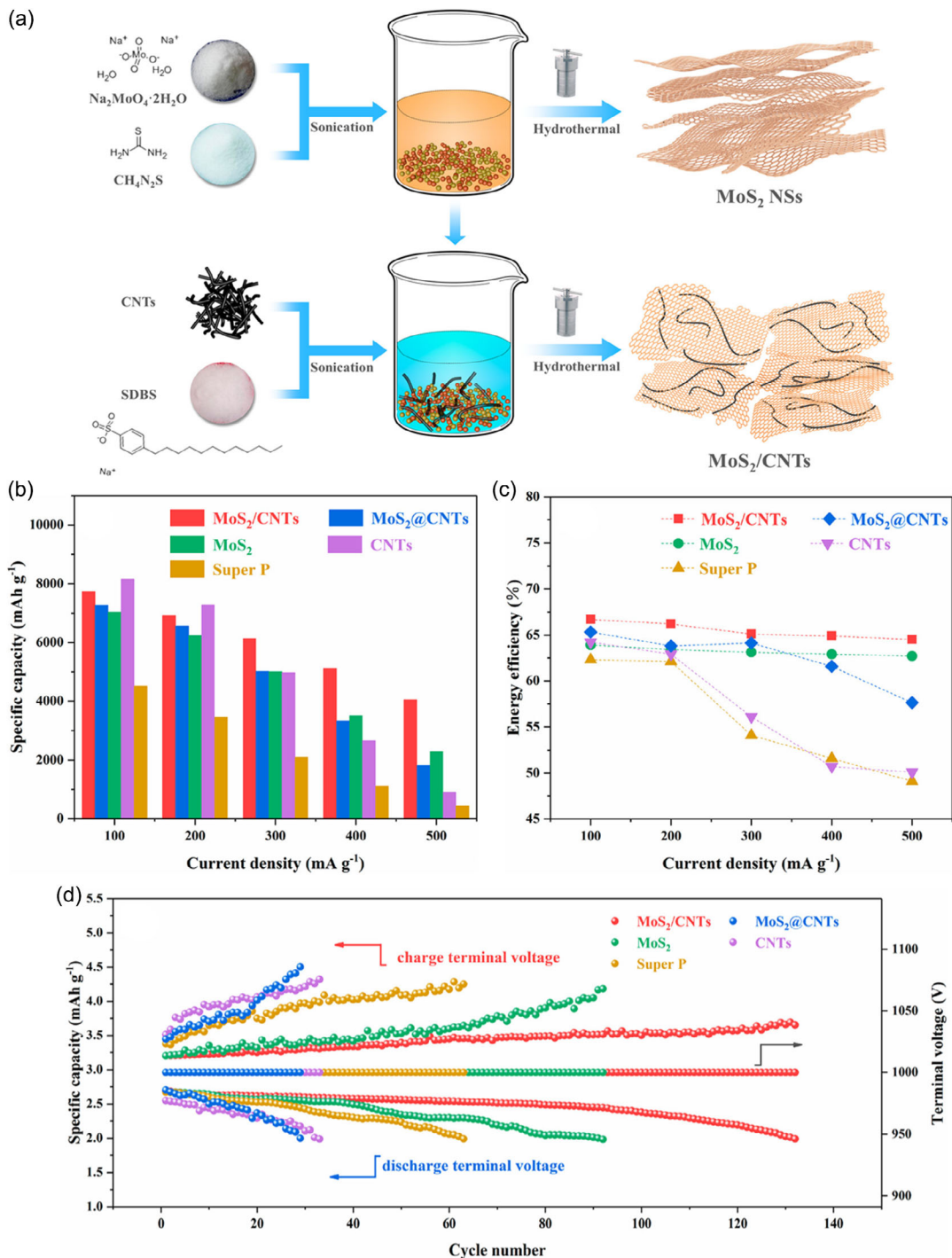


Figure 9. a) Scheme for the synthesis route of MoS₂/CNTs nanocomposites. Comparison of MoS₂/CNTs, MoS₂@CNTs, MoS₂, CNTs, and Super P-based Li–O₂ batteries in b) capacity and c) energy efficiency via different current densities. d) Cyclic performance of five different Li–O₂ batteries at a current density of 200 mA g⁻¹ and limited capacity of 1000 mA h g⁻¹. Reproduced with permission.^[189] Copyright 2018, American Chemical Society.

passivating carbamate group on the other end.^[196,197] The power conversion efficiency of the devices improved further to 20.7% because the DPB-clenched s-SWNTs acted as superior crystal

growth templates and grain boundary passivators. Even with these promising findings, more research could be conducted to further enhance the efficiency of solar cells.

4.1. Synergy of COF, CMPs, and Metal Organic Framework with CNTs for Advanced Energy Storage

4.1.1. COF

Research on the application of COFs in batteries is actively underway, and several well-organized review papers exist on this topic. However, this review aims to encompass recent studies involving the combined use of CNTs and COFs.

While extensive research has delved into the application of COFs in batteries, comprehensive review papers exist on this subject.^[198] However, this review uniquely incorporates recent studies focusing on the collaborative utilization of CNTs and COFs.

COFs have become the focal point of diverse investigations across various electrochemical applications. Their organic nature imparts tunable chemical characteristics and adaptable structures. The controlled design of oxidation–reduction active sites within COF precursors allows for precise regulation of density and location, offering the capability to modify the energy density of electrode materials. Additionally, the introduction of organic functionalities that enhance metal ion mobility can be intricately woven into the COF structure, addressing challenges associated with sluggish ion transport in batteries. Furthermore, functionalities facilitating interactions with sulfur can be seamlessly embedded in the COF backbone, augmenting sulfur loading and mitigating sulfur loss during charge–discharge cycles. The 2D layer structure of COFs, providing aligned 1D straight pores, simplifies ion movement and reduces resistance compared to complex interwoven pore channels. This 2D layer structure also affords the potential to control COF thickness, enabling access to the desired number of nanosheets in battery applications. Researchers have effectively harnessed these features to overcome challenges in battery applications, thereby significantly enhancing electrochemical performance.^[198]

In recent studies focusing on the application of CNT–COF composites, researchers have aimed to improve the performance of battery separators and cathodes. While lithium–sulfur batteries (LSBs) have garnered significant attention due to their high specific capacity, stability issues arising from volume expansion and the formation of lithium dendrites have posed challenges. Li et al. focused on the efficient design of a cathode for Li–CO₂ batteries by employing a COF with superior CO₂ absorption properties. Hybridizing COF with ruthenium coated CNTs resulted in an efficient cathode. The robust 1D channels in COF acted as diffusion pathways for CO₂ and lithium ions, enhancing the electrochemical reaction rate. Li–CO₂ batteries based on COF demonstrated an ultrahigh capacity of 27 348 at 200 mA g⁻¹, low overpotential of 1.24 V at the limit capacity of 1000 mAh g⁻¹, and improved rate capability, showing a slow voltage decay as the current density increased from 0.1 to 4 A g⁻¹. The COF-based battery also exhibited stable cycling performance, completing 200 cycles at a high current density of 1 A g⁻¹.^[199] In a different study, a boron/oxygen-codoped carbon (BOC) network derived from a COF was manufactured on the surface of CNTs through a precisely designed organic coupling reaction. This strategy allowed uniform doping of boron and oxygen heteroatoms throughout the porous carbon, facilitating enhanced chemical absorption of polysulfides and improving cyclic stability. The

resulting BOC@CNT with 68.5% sulfur content demonstrated outstanding lithium polysulfide absorption, exhibiting remarkable electrochemical performance as a cathode in LSBs. The composite showcased a large reversible capacity (1077 mA h g⁻¹ after 200 cycles at 0.2 C) and excellent cyclic stability (794 mA h g⁻¹) after 500 cycles at 1 C). This innovative approach of fabricating BOC networks from COF precursors provides a new paradigm for designing interfaces with uniform heteroatoms to achieve superior electrochemical performance.^[200]

4.1.2. CMPs

Research utilizing CMPs for energy storage applications continues to thrive, and there is a well-organized review article available on this topic.^[201] In light of this, we explored recent reports that integrate CNT and CMP, focusing on their combined application in the latest studies, with a prevalent emphasis on their use in supercapacitors.

In one study, three novel microporous COF polymers (TBN–TPE–CMPs) based on brominated TBN were synthesized using Sonogashira coupling. These polymers exhibit high thermal stability (505 °C), a substantial charge yield (68%), a large surface area (1150 m² g⁻¹), and a high total pore volume (1.426 cm³ g⁻¹), featuring pores of sizes 1.04 and 2.00 nm. The TBN–TPE–CMP material was blended with SWCNT to create TBN–CMP/SWCNT nanocomposites for use as electrodes in batteries. Among the three TBN–CMP/SWCNT composites, the TBN–Py–CMP/SWCNT electrode demonstrated the highest specific capacitance (430 F g⁻¹ at 0.5 A g⁻¹) and outstanding capacity retention (99.18% after 2000 cycles at 10 A g⁻¹). The exceptional performance of the TBN–Py–CMP/SWCNT electrode is attributed to the strong π-stacking interaction between TBN–Py–CMP and the highly conductive SWCNT.^[193] Lyu et al. showed the performance of fiber-shaped supercapacitors (FSCs), enhanced by employing a resurrection–Hartwig coupling reaction to synthesize a microporous COF (CMP) network. CNT fibers attached to a polytriphenylamine-based network (CNF@CMP) were successfully fabricated, exhibiting a high specific capacitance area (671.9 mF cm⁻² at 1 mA cm⁻²). All-solid-state symmetrical asymmetric CNF@PTPA FSCs, manufactured using PVA/H₃PO₄ as a gel electrolyte, displayed high specific area capacitance (398 mF cm⁻² at 0.28 mA cm⁻²), a maximum operating voltage of 1.4 V, and an energy density of 18.33 μWh cm⁻². Moreover, they demonstrated excellent flexibility and mechanical stability, maintaining 84.5% of the initial capacitance after 10 000 bending cycles.^[202]

The same team of researchers reported an improvement in the performance of capacitors using a composite made through a p-phenylenediamine linker (SACMP) obtained by the resurrection–Hartwig coupling reaction with a spirobifluorene bromide core and p-phenylenediamine linker. The composite, synthesized via a one-pot polymerization on MWCNTs, demonstrated a high specific capacitance of 594 F g⁻¹ at a current density of 1.0 A g⁻¹ when the MWCNT content was approximately 10 wt%, representing a 252% enhancement compared to SACMP's 236 F g⁻¹. The symmetrically assembled MWCNT@SACMP supercapacitor exhibited an efficient specific capacitance

of 254 F g^{-1} at 900 W kg^{-1} and an energy density of 28.53 Wh kg^{-1} . Furthermore, it maintained 84.38% of the initial capacitance after 6000 cycles.^[203]

4.1.3. Metal Organic Framework

Metal organic framework (MOFs), renowned for their remarkable porosity and functional nanomaterial characteristics, have attracted considerable attention in the development of battery electrodes. Nonetheless, as highlighted in the introduction, MOFs inherently act as electron insulators, limiting charge transfer in electrode materials and, consequently, compromising the efficiency of electrochemically active nanomaterials. To effectively address these challenges, the creation of hybrids incorporating MOFs and conductive materials like CNTs has emerged as a promising solution. Transition metal oxides exhibit promise as cathode materials for the next generation of LIBs. However, many oxides undergo significant volume changes during lithium insertion/extraction, resulting in diminished electrochemical performance and impeding practical implementation. MOFs, serving as hybrid porous materials composed of organic linkers and metal ions, stand as ideal precursors for producing metal oxides or carbon/nitrogen-doped metal oxides through nitration. The additional integration with CNTs can prevent the clustering of metal oxides, thereby enhancing both structural stability and electronic conductivity. Recent research examples suggest that these composite materials are not exclusively utilized in cathodes but are also extended to anodes and separators, highlighting their versatility across various battery components.^[204]

In this study, a novel functional separator coating was fabricated, composed of CNT-decorated zirconium metal-organic framework (PCN@CNT) featuring a catalytic cobalt-porphyrin linker (Co-PCN-222). The uniform dispersion of cobalt within the porphyrin linker, strong adsorption, and catalytic activity at nitrogen positions, coupled with the rapid electron conduction network provided by high-conductivity CNTs, significantly enhanced the polysulfide oxidation activity and effectively suppressed the shuttle effect. As a result, a Li–S battery utilizing the PCN@CNT-coated separator exhibited specific capacities of 1157 mAh g^{-1} at 0.1 C , excellent rate performance with 696 mAh g^{-1} at 2 C , and a low average capacity decay of 0.067% over 500 cycles at 1 C .^[205] Qian et al. developed a MnO-decorated nitrogen-doped carbon/CNT (MnO/N–C/CNT) composite to alleviate the shuttle effect in LSBs. This composite, coated on the separator as an N–C/CNT network, provides both conductivity and physical barriers. The polar MnO enhances the chemical adsorption and conversion rate of lithium polysulfides. Consequently, LSBs employing the MnO/N–C/CNT-modified separator, deliver a high specific capacity of 950 mAh g^{-1} at 0.5 C , with a low-capacity decay rate of 0.022% per cycle over 500 cycles. The significantly improved performance maintains stable cycle stability even with a high sulfur loading of 5.5 mg cm^{-2} demonstrating over 200 cycles of reliable cycling performance.^[206]

The fabrication of hybrid materials based on porous carbon can alleviate the volume change and poor thermal conductivity associated with silicon electrodes. Qiao et al. prepared a chain-like carbon cluster structure with a shell-like structure derived

from MOF-induced porous carbon acting as a protective shell surrounding silicon nanoparticle, and CNTs serving as connectors for the carbon shell. The unique structure of this composite enables more effective accommodation of volume expansion, and CNTs enhance overall stability and conductivity. As a result, the obtained composite demonstrates excellent rate capacity and improved cycle stability, achieving a capacity of 732 mA h g^{-1} at 2 A g^{-1} , with a retention rate of 72.3% even after 100 cycles at 1 A g^{-1} .^[207] Xu et al. synthesized NiO/CNTs-10, which exhibits the highest reversible capacity of 812 mAh g^{-1} even after 100 cycles at 100 mA g^{-1} . Cycling at 2 A g^{-1} maintains a stable capacity of 502 mAh g^{-1} even after 300 cycles. This structure aids in enhancing electron transfer capability and buffering volume expansion during the cycling process. The excellent electrochemical performance of the NiO/CNT composite is attributed to the 3D conductive network formed by porous NiO microspheres interconnected by CNTs.^[208] Co-NC@CNTs with a 3D interconnected conductive carbon network were synthesized, featuring Co-NC nanoparticles derived from ZIF-67. These particles possess rich Co catalytic sites for both oxygen reduction reaction and oxygen evolution reaction, with a fine/microporous structure. CNTs, serving as the carbon scaffold, enhance conductivity by facilitating electron transfer. The interconnected carbon network provides ample space for discharge products and prevents the deactivation of catalytically active sites. As a result, Co-NC@CNTs used as cathodic catalysts in lithium–oxygen batteries exhibit high initial discharge capacity ($12572.2 \text{ mA h g}^{-1}$) at 200 mA g^{-1} , excellent rate capability (5865 mA h g^{-1} at 1000 mA g^{-1}), and outstanding cycling stability (145 cycles at 250 mA g^{-1}). This study offers an effective design and manufacturing method to enhance the performance of lithium–oxygen batteries.^[209] To overcome the limitations of lithium–sulfur batteries, such as the shuttle effect of polysulfides, volume expansion, and the formation of lithium dendrites, Wang et al. developed a MOF-doping strategy. They constructed a hollow porous carbon framework with a surface shell composed of Ni, Co particles, and CNTs, termed Ni/Co-CNT/NHPC, to address stability issues and unstable rate characteristics. This porous framework enhances the sulfur loading, mitigates volume changes, and physically captures soluble polysulfides. The CNT-coated network structure is beneficial for optimizing material conductivity and porosity, accelerating reaction rates. Additionally, the abundant defects and interactions of Ni and Co nanoparticles strengthen the chemical adsorption of polysulfides, suppressing the shuttle effect. As a result, the Ni/Co-CNT/NHPC-S cathode achieves a high specific capacity (1352 mA h g^{-1}) and exhibits excellent cycle stability at 1 C , showing a low-capacity decay rate of 0.094% over 500 cycles.^[210]

5. Conclusion

As discussed above, CNTs have a variety of device applications owing to their desirable aspect ratio, chemical and mechanical stability, and metallic or semiconducting electronic properties depending on their chirality. However, from the perspective of energy-device applications, the lack of dispersibility is a critical limiting factor. Therefore, there has been great effort from both the industrial and academic sectors to improve the dispersibility

of CNTs by developing CNT dispersants to meet the needs of device applications. This review briefly discusses the fundamentals of CNTs concerning chirality, physical properties, and synthesis methods. Furthermore, we surveyed the contemporary CNT dispersants reported in 2015.

To disperse CNTs in water and aqueous solvents, a combination of hydrophobic and hydrophilic parts in the structures of the dispersants is essential. Hydrophobic sections, such as aromatic compounds and alkyl chains, adsorb on the sidewall of CNTs, whereas hydrophilic sections, such as ionic groups, interact with solvents, leading to repulsive dispersion. Dispersants for organic solvents also contain aromatic compounds which induce $\pi-\pi$ interactions with CNT surfaces. However, because organic solvents can be polar and nonpolar, a more subtle chemical design for dispersants is necessary. Although in aqueous solvents, the hydrophilic parts of CNT dispersants are combined at the end of the Gemini surfactant structure, dispersion is induced through steric hindrance by long alkyl groups. Nevertheless, if the structure of the dispersant becomes too bulky while the bonding strength with CNT improves, precipitation results from the weight of the dispersant + CNTs. Therefore, to apply dispersed CNTs to energy devices, particularly for dispersion in organic solvents, developing CNT dispersants with a simple structure and low molecular mass is warranted.

Keeping these observations in mind, if the goal is to develop energy devices that are commercially viable and ecologically sustainable, some major challenges to overcome are: 1) Develop CNT dispersion that is scalable for mass production because most proposed dispersion methods are validated in a laboratory setting without consideration for manufacturability. 2) Given that energy devices, such as household batteries, are usually mass produced with a significant ecological impact, the selection of a suitable dispersion method for such devices needs to take ecological sustainability into consideration. 3) CNT dispersion should demonstrate a significant advantage over other alternatives in the crowded space of candidate materials for next-generation energy devices.

It is expected that by addressing these challenges, further progress could be made to advance energy devices. Up until recently, the dominant trend among a limited number of studies is to apply CNT dispersion to energy storage devices. On the other hand, a novel contribution of the current review, in addition to recommendations for optimal dispersion in energy devices, is drawing more attention to energy conversion devices such as photovoltaic cells. Given that the spectrum of energy devices that benefit from dispersed CNTs is wider than is usually acknowledged, the domain of dispersion applications remains largely unexplored.

Acknowledgements

Y.J.C. and E.J.C.N. contributed equally to this work. The authors gratefully acknowledge the Japan Society for the Promotion of Science (JSPS) KAKENHI (grant no. JP23K04872). This work was supported by the National Research Foundation of Korea (NRF), funded by the Ministry of Science and ICT (MSIT) of the Korean government (grant nos. NRF-2021R1C1C1009200 and NRF-RS-2023-00220435, NRF-2023R1A2C3007358, NRF-RS-2023-00228994). The authors thank

Kyungshin Holdings and ENPLUS for their financial support. C.H. is financially supported by APC funding.

Conflict of Interest

The authors declare no conflict of interest.

Keywords

aqueous and organic solvents, carbon nanotubes, chirality, dispersants, dispersion, functionalization, synthesis methods

Received: October 9, 2023

Revised: December 11, 2023

Published online: January 24, 2024

- [1] B. Bhushan, in *Springer Handbook of Nanotechnology* (Ed: B. Bhushan), Springer Berlin Heidelberg, Berlin, Heidelberg **2017**, pp. 1–19.
- [2] A. K. Geim, K. S. Novoselov, In *Nanoscience and Technology*, Co-Published with Macmillan Publishers Ltd, London, UK **2009**, pp. 11–19.
- [3] H. W. Kroto, J. R. Heath, S. C. O'Brien, R. F. Curl, R. E. Smalley, *Nature* **1985**, 318, 162.
- [4] X. Xu, R. Ray, Y. Gu, H. J. Ploehn, L. Gearheart, K. Raker, W. A. Scrivens, *J. Am. Chem. Soc.* **2004**, 126, 12736.
- [5] S. Iijima, *Nature* **1991**, 354, 56.
- [6] Z. Spitalsky, D. Tasis, K. Papagelis, C. Galiotis, *Prog. Polym. Sci.* **2010**, 35, 357.
- [7] P. R. Bandaru, *J. Nanosci. Nanotechnol.* **2007**, 7, 1239.
- [8] J. N. Coleman, U. Khan, W. J. Blau, Y. K. Gun'ko, *Carbon* **2006**, 44, 1624.
- [9] R. R. Bacsa, C. Laurent, A. Peigney, W. S. Bacsa, T. Vaugien, A. Rousset, *Chem. Phys. Lett.* **2000**, 323, 566.
- [10] L. Zhu, J. Xu, Y. Xiu, Y. Sun, D. W. Hess, C. P. Wong, *Carbon* **2006**, 44, 253.
- [11] F. Deng, Q.-S. Zheng, *Appl. Phys. Lett.* **2008**, 92, 071902.
- [12] T. Lee, K. T. Park, B.-C. Ku, H. Kim, *Nanoscale* **2019**, 11, 16919.
- [13] M. Fujii, X. Zhang, H. Xie, H. Ago, K. Takahashi, T. Ikuta, H. Abe, T. Shirizawa, *Phys. Rev. Lett.* **2005**, 95, 65502.
- [14] J.-P. Salvetat, J.-M. Bonard, N. H. Thomson, A. J. Kulik, L. Forró, W. Benoit, L. Zuppiroli, *Appl. Phys. A* **1999**, 69, 255.
- [15] J. Liu, M. J. Casavant, M. Cox, D. A. Walters, P. Boul, W. Lu, A. J. Rimberg, K. A. Smith, D. T. Colbert, R. E. Smalley, *Chem. Phys. Lett.* **1999**, 303, 125.
- [16] C. de las Casas, W. Li, *J. Power Sources* **2012**, 208, 74.
- [17] Q. Zhao, Z. Gan, Q. Zhuang, *Electroanalysis* **2002**, 14, 1609.
- [18] H. Dai, A. L. I. Javey, E. Pop, D. Mann, W. Kim, Y. Lu, *Nano* **2006**, 1, 1.
- [19] X.-M. Liu, Z. D. Huang, S. W. Oh, B. Zhang, P.-C. Ma, M. M. F. Yuen, J.-K. Kim, *Compos. Sci. Technol.* **2012**, 72, 121.
- [20] M. Mohamed Samy, M. Gamal Mohamed, A. F. M. EL-Mahdy, T. Hassan Mansoure, K. C.-W. Wu, S.-W. Kuo, *ACS Appl. Mater. Interfaces* **2021**, 13, 51906.
- [21] C. Liu, Y. Y. Fan, M. Liu, H. T. Cong, H. M. Cheng, M. S. Dresselhaus, *Science* **1999**, 286, 1127.
- [22] L. Wen, F. Li, H.-M. Cheng, *Adv. Mater.* **2016**, 28, 4306.
- [23] N. B. Saleh, L. D. Pfefferle, M. Elimelech, *Environ. Sci. Technol.* **2008**, 42, 7963.
- [24] Q. Yang, X. He, X. Liu, F. Leng, Y.-W. Mai, *Composites, Part B* **2012**, 43, 33.

- [25] P.-C. Ma, N. A. Siddiqui, G. Marom, J.-K. Kim, *Composites, Part A* **2010**, *41*, 1345.
- [26] M. Faisal, M. A. Hannan, P. J. Ker, A. Hussain, M. B. Mansor, F. Blaabjerg, *IEEE Access* **2018**, *6*, 35143.
- [27] Y. Zhao, O. Pohl, A. I. Bhatt, G. E. Collis, P. J. Mahon, T. Rüther, A. F. Hollenkamp, *Sustainable Chem.* **2021**, *2*, 167.
- [28] L.-F. Cui, L. Hu, J. W. Choi, Y. Cui, *ACS Nano* **2010**, *4*, 3671.
- [29] X. Jin, H. Huang, A. Wu, S. Gao, M. Lei, J. Zhao, X. Gao, G. Cao, *ACS Nano* **2018**, *12*, 8037.
- [30] S. H. Ng, J. Wang, Z. P. Guo, J. Chen, G. X. Wang, H. K. Liu, *Electrochim. Acta* **2005**, *51*, 23.
- [31] L. G. Bulusheva, A. V. Okotrub, A. G. Kurenya, H. Zhang, H. Zhang, X. Chen, H. Song, *Carbon* **2011**, *49*, 4013.
- [32] J. Liu, K. Li, Q. Zhang, X. Zhang, X. Liang, J. Yan, H. H. Tan, Y. Yu, Y. Wu, *ACS Appl. Mater. Interfaces* **2021**, *13*, 45547.
- [33] X. -M. Fan, X. -H Zhang, G. -R. Hu, B. Zhang, Z. -J. He, Y. -J. Li, J. -C. Zheng, *Ionics* **2020**, *26*, 1721.
- [34] K. Jin, X. Zhou, L. Zhang, X. Xin, G. Wang, Z. Liu, *J. Phys. Chem. C* **2013**, *117*, 21112.
- [35] J. Asenbauer, T. Eisenmann, M. Kuenzel, A. Kazzazi, Z. Chen, D. Bresser, *Sustainable Energy Fuels* **2020**, *4*, 5387.
- [36] A. Di Crescenzo, V. Ettorre, A. Fontana, *Beilstein J. Nanotechnol.* **2014**, *5*, 1675.
- [37] O. V. Kharissova, B. I. Kharisov, E. G. De Casas Ortiz, *Dispersion of Carbon Nanotubes in Water and Non-Aqueous Solvents*, Vol. 3, Royal Society of Chemistry **2013**, pp. 24812–24852.
- [38] D. R. Dreyer, R. S. Ruoff, C. W. Bielawski, *Angew. Chem., Int. Ed.* **2010**, *49*, 9336.
- [39] A. K.-T. Lau, D. Hui, *Composites, Part B* **2002**, *33*, 263.
- [40] T. W. Ebbesen, H. J. Lezec, H. Hiura, J. W. Bennett, H. F. Ghaemi, T. Thio, *Nature* **1996**, *382*, 54.
- [41] Z. Torbatian, R. Asgari, *Appl. Sci.* **2018**, *8*, 238.
- [42] E. A. Laird, F. Kuemmeth, G. A. Steele, K. Grove-Rasmussen, J. Nygård, K. Flensberg, L. P. Kouwenhoven, *Rev. Mod. Phys.* **2015**, *87*, 703.
- [43] J.-C. Charlier, *Acc. Chem. Res.* **2002**, *35*, 1063.
- [44] A. Agresti, A. Pazniak, S. Pescetelli, A. Di Vito, D. Rossi, A. Pecchia, M. Auf der Maur, A. Liedl, R. Larciprete, D. V. Kuznetsov, D. Saranin, A. Di Carlo, *Nat. Mater.* **2019**, *18*, 1228.
- [45] M. R. Oduncu, Z. Ke, B. Zhao, Z. Shang, R. Simpson, H. Wang, A. Wei, *ACS Appl. Nano Mater.* **2023**, *6*, 14574.
- [46] Y. Hou, J. Tang, H. Zhang, C. Qian, Y. Feng, J. Liu, *ACS Nano* **2009**, *3*, 1057.
- [47] S. Rathinavel, K. Priyadarshini, D. Panda, *Mater. Sci. Eng. B* **2021**, *268*, 115095.
- [48] Q. Zhang, W. Zhou, X. Xia, K. Li, N. Zhang, Y. Wang, Z. Xiao, Q. Fan, E. I. Kauppinen, S. Xie, *Adv. Mater.* **2020**, *32*, 2004277.
- [49] I. Jeon, T. Chiba, C. Delacou, Y. Guo, A. Kaskela, O. Reynaud, E. I. Kauppinen, S. Maruyama, Y. Matsuo, *Nano Lett.* **2015**, *15*, 6665.
- [50] I. Jeon, R. Xiang, A. Shawky, Y. Matsuo, S. Maruyama, *Adv. Energy Mater.* **2019**, *9*, 1801312.
- [51] I. Jeon, K. Cui, T. Chiba, A. Anisimov, A. G. Nasibulin, E. I. Kauppinen, S. Maruyama, Y. Matsuo, *J. Am. Chem. Soc.* **2015**, *137*, 7982.
- [52] I. Jeon, J. Yoon, U. Kim, C. Lee, R. Xiang, A. Shawky, J. Xi, J. Byeon, H. M. Lee, M. Choi, S. Maruyama, Y. Matsuo, *Adv. Energy Mater.* **2019**, *9*, 1901204.
- [53] J.-M. Choi, J. Han, T. Rane, S. Kim, I. S. Kim, I. Jeon, *J. Phys.: Energy* **2022**, *4*, 042004.
- [54] H.-S. Lin, S. Okawa, Y. Ma, S. Yotsumoto, C. Lee, S. Tan, S. Manzhos, M. Yoshizawa, S. Chiashi, H. M. Lee, T. Tanaka, H. Kataura, I. Jeon, Y. Matsuo, S. Maruyama, *Chem. Mater.* **2020**, *32*, 5125.
- [55] S. Seo, I. Jeon, R. Xiang, C. Lee, H. Zhang, T. Tanaka, J.-W. Lee, D. Suh, T. Ogamoto, R. Nishikubo, A. Saeki, S. Chiashi, J. Shiomi, H. Kataura, H. M. Lee, Y. Yang, Y. Matsuo, S. Maruyama, *J. Mater. Chem. A* **2019**, *7*, 12987.
- [56] S. Rols, A. Righi, L. Alvarez, E. Anglaret, R. Almairac, C. Journet, P. Bernier, J. L. Sauvajol, A. M. Benito, W. K. Maser, E. Muñoz, M. T. Martinez, G. F. de laFuente, A. Girard, J. C. Ameline, *Eur. Phys. J. B* **2000**, *18*, 201.
- [57] S. Bandow, S. Asaka, Y. Saito, A. M. Rao, L. Grigorian, E. Richter, P. C. Eklund, *Phys. Rev. Lett.* **1998**, *80*, 3779.
- [58] W. Ren, H.-M. Cheng, *J. Phys. Chem. B* **2005**, *109*, 7169.
- [59] A. Grüneis, M. H. Rümmeli, C. Kramberger, A. Barreiro, T. Pichler, R. Pfeiffer, H. Kuzmany, T. Gemming, B. Büchner, *Carbon* **2006**, *44*, 3177.
- [60] Ossila, *Carbon Nanotubes*, <https://www.ossila.com/en-kr/collections/carbon-nanotubes> (accessed: January 2022).
- [61] F. Li, H. M. Cheng, S. Bai, G. Su, M. S. Dresselhaus, *Appl. Phys. Lett.* **2000**, *77*, 3161.
- [62] Y. Cheng, X. Li, H. Gao, J. Wang, G. Luo, D. Golberg, M.-S. Wang, *Carbon* **2020**, *160*, 98.
- [63] A. H. Barber, R. Andrews, L. S. Schadler, H. D. Wagner, *Appl. Phys. Lett.* **2005**, *87*, 203106.
- [64] J.-Y. Hsieh, J.-M. Lu, M.-Y. Huang, C.-C. Hwang, *Nanotechnology* **2006**, *17*, 3920.
- [65] X. Wei, Q. Chen, L.-M. Peng, R. Cui, Y. Li, *J. Phys. Chem. C* **2009**, *113*, 17002.
- [66] M. F. Yu, O. Lourie, M. J. Dyer, K. Moloni, T. F. Kelly, R. S. Ruoff, *Science* **2000**, *287*, 637.
- [67] Z. L. Wang, D. W. Tang, X. H. Zheng, W. G. Zhang, Y. T. Zhu, *Nanotechnology* **2007**, *18*, 475714.
- [68] R. Prasher, *Phys. Rev. B* **2008**, *77*, 75424.
- [69] Y.-H. Li, J. Wei, X. Zhang, C. Xu, D. Wu, L. Lu, B. Wei, *Chem. Phys. Lett.* **2002**, *365*, 95.
- [70] J. Wei, H. Zhu, B. Jiang, L. Ci, D. Wu, *Carbon* **2003**, *41*, 2495.
- [71] C. L. Kane, E. J. Mele, R. S. Lee, J. E. Fischer, P. Petit, H. Dai, A. Thess, R. E. Smalley, A. R. M. Verschueren, S. J. Tans, C. Dekker, *Europhys. Lett.* **1998**, *41*, 683.
- [72] A. Di Crescenzo, M. Aschi, E. Del Canto, S. Giordani, D. Demurtas, A. Fontana, *Phys. Chem. Chem. Phys.* **2011**, *13*, 11373.
- [73] Y. Wang, Z. Iqbal, S. Mitra, *J. Am. Chem. Soc.* **2005**, *128*, 95.
- [74] S. Detriche, J. B. Nagy, Z. Mekhalif, J. Delhalle, *J. Nanosci. Nanotechnol.* **2009**, *9*, 6015.
- [75] J. A. Baker, C. Worsley, H. K. H. Lee, R. N. Clark, W. C. Tsoi, G. Williams, D. A. Worsley, D. T. Gethin, T. M. Watson, *Adv. Eng. Mater.* **2017**, *19*, 1600652.
- [76] K. L. Ng, B. M. Maciejewska, L. Qin, C. Johnston, J. Barrio, M.-M. Titirici, I. Tzanakis, D. G. Eskin, K. Porfyrakis, J. Mi, N. Grobert, *ACS Sustainable Chem. Eng.* **2023**, *11*, 58.
- [77] A. O'Neill, U. Khan, P. N. Nirmalraj, J. Boland, J. N. Coleman, *J. Phys. Chem. C* **2011**, *115*, 5422.
- [78] M. Wang, M. Jin, C. Chen, F. Li, Y. Rong, R. Liu, H. Li, Y. Feng, Z. Shen, *Sol. RRL* **2022**, *6*, 2200710.
- [79] K. Maleski, V. N. Mochalin, Y. Gogotsi, *Chem. Mater.* **2017**, *29*, 1632.
- [80] T. Chen, G. Tong, E. Xu, H. Li, P. Li, Z. Zhu, J. Tang, Y. Qi, Y. Jiang, *J. Mater. Chem. A* **2019**, *7*, 20597.
- [81] M. Chernysheva, A. Rozhin, Y. Fedotov, C. Mou, R. Arif, S. M. Koblsev, E. M. Dianov, S. K. Turitsyn, *Nanophotonics* **2017**, *6*, 1.
- [82] M. Kundrapu, J. Li, A. Shashurin, M. Keidar, *J. Phys. D: Appl. Phys.* **2012**, *45*, 315305.
- [83] N. Arora, N. N. Sharma, *Diamond Relat. Mater.* **2014**, *50*, 135.
- [84] E. G. Gamaly, T. W. Ebbesen, *Phys. Rev. B* **1995**, *52*, 2083.
- [85] M. Keidar, *J. Phys. D: Appl. Phys.* **2007**, *40*, 2388.
- [86] M. Keidar, A. M. Waas, *Nanotechnology* **2004**, *15*, 1571.

- [87] A. V. Krestinin, N. A. Kiselev, A. V. Raevskii, A. G. Ryabenko, D. N. Zakharov, G. I. Zvereva, *Eurasian Chem. Technol. J.* **2003**, 5, 7.
- [88] Y. Su, Y. Zhang, H. Wei, B. Qian, Z. Yang, Y. Zhang, *Phys. E* **2012**, 44, 1548.
- [89] O. Volotskova, I. Levchenko, A. Shashurin, Y. Raitses, K. Ostrikov, M. Keidar, *Nanoscale* **2010**, 2, 2281.
- [90] O. Volotskova, J. A. Fagan, J. Yeon Huh, F. R. Phelan Jr., A. Shashurin, M. Keidar, *ACS Nano* **2010**, 4, 5187.
- [91] M. Keidar, I. Levchenko, T. Arbel, M. Alexander, A. M. Waas, K. Ostrikov, *Appl. Phys. Lett.* **2008**, 92, 043129.
- [92] Y. Su, Y. Zhang, H. Wei, Z. Yang, E. S.-W. Kong, Y. Zhang, *Carbon* **2012**, 50, 2556.
- [93] M. S. Roslan, K. T. Chaudhary, N. Doylend, A. Agam, R. Kamarulzaman, Z. Haider, E. Mazalan, J. Ali, *J. Saudi Chem. Soc.* **2019**, 23, 171.
- [94] T. Guo, P. Nikolaev, A. Thess, D. T. Colbert, R. E. Smalley, *Chem. Phys. Lett.* **1995**, 243, 49.
- [95] T. Guo, P. Nikolaev, A. G. Rinzler, D. Tomanek, D. T. Colbert, R. E. Smalley, *J. Phys. Chem.* **1995**, 99, 10694.
- [96] C. D. Scott, S. Areppalli, P. Nikolaev, R. E. Smalley, *Appl. Phys. A: Mater. Sci. Process.* **2001**, 72, 573.
- [97] J. Chrzanowska, J. Hoffman, A. Małolepszy, M. Mazurkiewicz, T. A. Kowalewski, Z. Szymanski, L. Stobinski, *Phys. Status Solidi B* **2015**, 252, 1860.
- [98] M. Yudasaka, F. Kokai, K. Takahashi, R. Yamada, N. Sensui, T. Ichihashi, S. Iijima, *J. Phys. Chem. B* **1999**, 103, 3576.
- [99] M. Yudasaka, R. Yamada, N. Sensui, T. Wilkins, T. Ichihashi, S. Iijima, *J. Phys. Chem. B* **1999**, 103, 6224.
- [100] Y. Zhang, H. Gu, S. Iijima, *Appl. Phys. Lett.* **1998**, 73, 3827.
- [101] C. Journet, P. Bernier, *Appl. Phys. A* **1998**, 67, 1.
- [102] Y. Zhang, S. Iijima, *Appl. Phys. Lett.* **1999**, 75, 3087.
- [103] C. Shen, A. H. Brozena, Y. Wang, *Nanoscale* **2011**, 3, 503.
- [104] R. A. Ismail, M. H. Mohsin, A. K. Ali, K. I. Hassoon, S. Erten-Ela, *Phys. E* **2020**, 119, 113997.
- [105] S. B. Sinnott, R. Andrews, D. Qian, A. M. Rao, Z. Mao, E. C. Dickey, F. Derbyshire, *Chem. Phys. Lett.* **1999**, 315, 25.
- [106] A. Magrez, J. W. Seo, R. Smajda, M. Mionić, L. Forró, *Materials* **2010**, 3, 4871.
- [107] S. H. Lee, J. Park, J. H. Park, D. M. Lee, A. Lee, S. Y. Moon, S. Y. Lee, H. S. Jeong, S. M. Kim, *Carbon* **2021**, 173, 901.
- [108] B. Mclean, E. I. Kauppinen, A. J. Page, *J. Appl. Phys.* **2021**, 129, 044302.
- [109] S. Y. Moon, S. Y. Jeon, S. H. Lee, A. Lee, S. M. Kim, *Nanomaterials* **2022**, 12, 863.
- [110] S. Y. Moon, B. R. Kim, C. W. Park, S. H. Lee, S. M. Kim, *Chem. Eng. J. Adv.* **2022**, 10, 100261.
- [111] T. Kinoshita, M. Karita, N. Chikyu, T. Nakano, Y. Inoue, *Carbon* **2022**, 196, 391.
- [112] P. Nikolaev, M. J. Bronikowski, R. K. Bradley, F. Rohrmund, D. T. Colbert, K. A. Smith, R. E. Smalley, *Chem. Phys. Lett.* **1999**, 313, 91.
- [113] M. L. Healy, L. J. Dahlben, J. A. Isaacs, *J. Ind. Ecol.* **2008**, 12, 376.
- [114] M. Musaddique, A. Rafique, J. Iqbal, *J. Encapsulation Adsorpt. Sci.* **2011**, 1, 29.
- [115] J. Hou, W. Du, C. Zhao, X. Du, Z. Wang, S. Li, K. Liu, *Mater. Chem. Phys.* **2019**, 229, 279.
- [116] S. D. Bergin, Z. Sun, D. Rickard, P. V. Streich, J. P. Hamilton, J. N. Coleman, *ACS Nano* **2009**, 3, 2340.
- [117] A. Bor, B. Ichinkhorloo, B. Uyanga, J. Lee, H. Choi, *Powder Technol.* **2018**, 323, 563.
- [118] B. J. Kim, S. Y. Oh, H. S. Yun, J. H. Ki, C. J. Kim, S. Baik, B. S. Lim, *J. Nanosci. Nanotechnol.* **2009**, 9, 7393.
- [119] N. S. Anas, M. Ramakrishna, R. Vijay, *Met. Mater. Int.* **2020**, 26, 272.
- [120] W. Steinmann, T. Vad, B. Weise, J. Wulfhorst, G. Seide, T. Gries, M. Heidelmann, T. Weirich, *Polym. Polym. Compos.* **2013**, 21, 473.
- [121] A. Jiménez-Suárez, M. Campo, I. Gaztelumendi, N. Markaide, M. Sánchez, A. Ureña, *Composites, Part B* **2013**, 48, 88.
- [122] P. Y. Zhai, J. Q. Huang, L. Zhu, J. Le Shi, W. Zhu, Q. Zhang, *Carbon* **2017**, 111, 493.
- [123] A. Hirsch, *Angew. Chem., Int. Ed.* **2002**, 41, 1628.
- [124] A. Hirsch, O. Vostrowsky, *Top. Curr. Chem.* **2005**, 245, 193.
- [125] W. Huang, S. Taylor, K. Fu, Y. Lin, D. Zhang, T. W. Hanks, A. M. Rao, Y. P. Sun, *Nano Lett.* **2002**, 2, 311.
- [126] J. Čech, S. A. Curran, D. Zhang, J. L. Dewald, A. Avadhanula, M. Kandadai, S. Roth, *Phys. Status Solidi B* **2006**, 243, 3221.
- [127] J. K. Lim, W. S. Yun, M. Han Yoon, S. K. Lee, C. H. Kim, K. Kim, S. K. Kim, *Synth. Met.* **2003**, 139, 521.
- [128] P. C. Ma, J. K. Kim, B. Z. Tang, *Carbon* **2006**, 44, 3232.
- [129] L. G. Bulusheva, Y. V. Fedoseeva, E. Flahaut, J. Rio, C. P. Ewels, V. O. Koroteev, G. Van Lier, D. V. Vyalikh, A. V. Okotrub, *Beilstein J. Nanotechnol.* **2017**, 8, 1688.
- [130] L. G. Bulusheva, Yu. V. Fedoseeva, A. V. Okotrub, E. Flahaut, I. P. Asanov, V. O. Koroteev, A. Yaya, C. P. Ewels, A. L. Chuvilin, A. Felten, G. Van Lier, D. V. Vyalikh, *Chem. Mater.* **2010**, 22, 4197.
- [131] M. Adamska, U. Narkiewicz, *J. Fluorine Chem.* **2017**, 200, 179.
- [132] J. S. Im, S. C. Kang, B. C. Bai, T. S. Bae, S. J. In, E. Jeong, S. H. Lee, Y. S. Lee, *Carbon* **2011**, 49, 2235.
- [133] L. G. Bulusheva, V. I. Sysoev, E. V. Lobiak, Y. V. Fedoseeva, A. A. Makarova, M. Dubois, E. Flahaut, A. V. Okotrub, *Carbon* **2019**, 148, 413.
- [134] L. Moradi, I. Etesami, *Fuller. Nanotub. Carbon Nanostructures* **2016**, 24, 213.
- [135] L. G. Bulusheva, A. V. Okotrub, E. Flahaut, I. P. Asanov, P. N. Gevko, V. O. Koroteev, Yu. V. Fedoseeva, A. Yaya, C. P. Ewels, *Chem. Mater.* **2012**, 24, 2708.
- [136] J. F. Colomer, R. Marega, H. Traboulisi, M. Meneghetti, G. Van Tendeloo, D. Bonifazi, *Chem. Mater.* **2009**, 21, 4747.
- [137] G. Zhang, P. Qi, X. Wang, Y. Lu, D. Mann, X. Li, H. Dai, *J. Am. Chem. Soc.* **2006**, 128, 6026.
- [138] S. Pekker, J.-P. Salvetat, E. Jakab, J.-M. Bonard, L. Forró, *ACS Publ. 2001*, 105, 7938.
- [139] A. Nikitin, H. Ogasawara, D. Mann, R. Denecke, Z. Zhang, H. Dai, K. Cho, A. Nilsson, *Phys. Rev. Lett.* **2005**, 95, 225507.
- [140] M. Vizuete, M. Barrejón, M. J. Gómez-Escalona, F. Langa, *Nanoscale* **2012**, 4, 4370.
- [141] W. H. Duan, Q. Wang, F. Collins, *Chem. Sci.* **2011**, 2, 1407.
- [142] M. Suttipong, N. R. Tummala, B. Kitiyanan, A. Striolo, *J. Phys. Chem. C* **2011**, 115, 17286.
- [143] M. D. Clark, S. Subramanian, R. Krishnamoorti, *J. Colloid Interface Sci.* **2011**, 354, 144.
- [144] S. M. Fatemi, M. Foroutan, *J. Iran. Chem. Soc.* **2015**, 12, 1905.
- [145] R. M. F. Fernandes, B. Abreu, B. Claro, M. Buzaglo, O. Regev, I. Furó, E. F. Marques, *Langmuir* **2015**, 31, 10955.
- [146] X. Xin, J. Pang, W. Li, Y. Wang, J. Yuan, G. Xu, *J. Surfactants Deterg.* **2015**, 18, 163.
- [147] G. F. Bass, M. S. Colt, A. D. Chavez, G. X. Dehoe, T. P. Formal, C. P. Seaver, K. Kha, B. A. Kelley, G. E. Scott, C. E. Immoos, P. J. Costanzo, *Polymer* **2015**, 72, 301.
- [148] A. Mohamed, A. K. Anas, S. A. Bakar, T. Ardyani, W. M. W. Zin, S. Ibrahim, M. Sagisaka, P. Brown, J. Eastoe, *J. Colloid Interface Sci.* **2015**, 455, 179.
- [149] H. Cui, X. Yan, M. Monasterio, F. Xing, *Nanomaterials* **2017**, 7, 262.
- [150] M. Qiao, Q. Ran, S. Wu, *Appl. Surf. Sci.* **2018**, 433, 975.
- [151] Y. Li, H. Wei, L. Li, J. Wang, X. Qian, L. He, X. Wang, Q. Ouyang, Y. Chen, Y. Zhang, Y. Li, *J. Nanopart. Res.* **2018**, 20, 1.
- [152] F. M. Menger, J. S. Keiper, *Angew. Chem., Int. Ed.* **2000**, 39, 1906.

- [153] J. Hou, W. Du, F. Meng, C. Zhao, X. Du, *J. Colloid Interface Sci.* **2018**, 512, 750.
- [154] E. M. Sadek, D. E. El-Nashar, A. A. Ward, S. M. Ahmed, *J. Polym. Res.* **2018**, 25, 1.
- [155] B. Abreu, J. Rocha, R. M. F. Fernandes, O. Regev, I. Furó, E. F. Marques, *J. Colloid Interface Sci.* **2019**, 547, 69.
- [156] P. Zhang, T. Zhou, L. He, S. Zhang, J. Sun, J. Wang, C. Qin, L. Dai, *RSC Adv.* **2015**, 5, 55492.
- [157] Z. Li, T. Kameda, T. Isoshima, E. Kobatake, T. Tanaka, Y. Ito, M. Kawamoto, *Langmuir* **2015**, 31, 3482.
- [158] P. Zhu, Y. Liu, Z. Fang, Y. Kuang, Y. Zhang, C. Peng, G. Chen, *Langmuir* **2019**, 35, 4834.
- [159] F. Toshimitsu, W. Ishimaru, N. Nakashima, *Bull. Chem. Soc. Jpn.* **2019**, 92, 1679.
- [160] H. Chaudhary, R. M. F. Fernandes, V. Gowda, M. M. A. E. Claessens, I. Furó, C. Lendel, *J. Colloid Interface Sci.* **2019**, 556, 172.
- [161] H. Zhao, L. Guo, Y. Lian, *RSC Adv.* **2020**, 10, 21643.
- [162] T. Lee, B. Kim, S. Kim, J. H. Han, H. B. Jeon, Y. S. Lee, H. J. Paik, *Nanoscale* **2015**, 7, 6745.
- [163] T. Lee, J. Park, K. Kim, A. K. Mohanty, B. Kim, J. H. Han, H. B. Jeon, Y. S. Lee, H. J. Paik, *RSC Adv.* **2015**, 5, 69410.
- [164] Z. Deng, H. Yu, L. Wang, X. Zhai, *J. Organomet. Chem.* **2015**, 791, 274.
- [165] C. Liu, B. Liu, M. B. Chan-Park, *Polym. Chem.* **2017**, 8, 674.
- [166] C. Liang, B. Wang, J. Chen, Q. Yong, Y. Huang, B. Liao, *J. Phys. Chem. B* **2017**, 121, 8408.
- [167] D. Fong, Z. Hua, T. R. Wilks, R. K. O'Reilly, A. Adronov, *J. Polym. Sci., Part A: Polym. Chem.* **2017**, 55, 2611.
- [168] F. Faraguna, R. Blažić, E. Vidović, A. Jukić, *React. Funct. Polym.* **2022**, 177, 105315.
- [169] X. Zhang, M. Kah, M. T. O. Jonker, T. Hofmann, *Environ. Sci. Technol.* **2012**, 46, 7166.
- [170] N. Nakashima, Y. Tomonari, H. Murakami, *Chem. Lett.* **2002**, 638.
- [171] K. C. Etika, F. D. Jochum, P. Theato, J. C. Grunlan, *J. Am. Chem. Soc.* **2009**, 131, 13598.
- [172] C. Backes, U. Mundloch, A. Ebel, F. Hauke, A. Hirsch, *Chem. Eur. J.* **2010**, 16, 3314.
- [173] Y. Wang, M. Liu, T. Liu, D. Lu, Y. Sun, H. Zhang, Z. Jiang, *Compos. Sci. Technol.* **2017**, 143, 82.
- [174] K. Li, V. Kardelis, A. Adronov, *J. Polym. Sci., Part A: Polym. Chem.* **2018**, 56, 2053.
- [175] D. Xu, T. A. P. Seery, Y. Gao, L. Ding, C. Zhou, Z. Wang, Z. Jiang, H. Zhang, *J. Appl. Polym. Sci.* **2020**, 137, 48379.
- [176] Z. Yang, J. Tian, Z. Yin, C. Cui, W. Qian, F. Wei, *Carbon* **2019**, 141, 467.
- [177] M. G. Mohamed, W.-C. Chen, A. F. M. EL-Mahdy, S.-W. Kuo, *J. Polym. Res.* **2021**, 28, 219.
- [178] M. G. Mohamed, M. M. Samy, T. H. Mansoure, C.-J. Li, W.-C. Li, J.-H. Chen, K. Zhang, S.-W. Kuo, *Int. J. Mol. Sci.* **2022**, 23, 347.
- [179] B.-S. Lou, P. Veerakumar, S.-M. Chen, V. Veeramani, R. Madhu, S.-B. Liu, *Sci. Rep.* **2016**, 6, 19949.
- [180] L. Sun, X. Wang, Y. Wang, Q. Zhang, *Carbon* **2017**, 122, 462.
- [181] L. Hu, J. W. Choi, Y. Yang, S. Jeong, F. La Mantia, L.-F. Cui, Y. Cui, *Proc. Natl. Acad. Sci.* **2009**, 106, 21490.
- [182] J. Jiang, Y. Li, J. Liu, X. Huang, C. Yuan, X. W. D. Lou, *Adv. Mater.* **2012**, 24, 5166.
- [183] X. Wang, X. Lu, B. Liu, D. Chen, Y. Tong, G. Shen, *Adv. Mater.* **2014**, 26, 4763.
- [184] P. Poizot, S. Laruelle, S. Grugéon, L. Dupont, J.-M. Tarascon, *Nature* **2000**, 407, 496.
- [185] Y. Gong, D. Li, C. Luo, Q. Fu, C. Pan, *Green Chem.* **2017**, 19, 4132.
- [186] S. Y. Chew, S. H. Ng, J. Wang, P. Novák, F. Krumeich, S. L. Chou, J. Chen, H. K. Liu, *Carbon* **2009**, 47, 2976.
- [187] F. Pan, J. Wang, Z. Yang, L. Gu, Y. Yu, *RSC Adv.* **2015**, 5, 77518.
- [188] S. M. Abbas, S. T. Hussain, S. Ali, N. Ahmad, N. Ali, S. Abbas, *J. Mater. Sci.* **2013**, 48, 5429.
- [189] A. Hu, J. Long, C. Shu, R. Liang, J. Li, *ACS Appl. Mater. Interfaces* **2018**, 10, 34077.
- [190] O. Toprakci, H. A. K. Toprakci, L. Ji, G. Xu, Z. Lin, X. Zhang, *ACS Appl. Mater. Interfaces* **2012**, 4, 1273.
- [191] Z. Wu, X. Han, J. Zheng, Y. Wei, R. Qiao, F. Shen, J. Dai, L. Hu, K. Xu, Y. Lin, W. Yang, F. Pan, *Nano Lett.* **2014**, 14, 4700.
- [192] M. M. Samy, M. G. Mohamed, S.-W. Kuo, *Compos. Sci. Technol.* **2020**, 199, 108360.
- [193] M. M. Samy, M. G. Mohamed, A. F. M. EL-Mahdy, T. H. Mansoure, K. C.-W. Wu, S.-W. Kuo, *ACS Appl. Mater. Interfaces* **2021**, 13, 51906.
- [194] M. G. Mohamed, M. M. Samy, T. H. Mansoure, S. U. Sharma, M.-S. Tsai, J.-H. Chen, J.-T. Lee, S.-W. Kuo, *ACS Appl. Energy Mater.* **2022**, 5, 3677.
- [195] H.-S. Lin, S. Okawa, Y. Ma, S. Yotsumoto, C. Lee, S. Tan, S. Manzhos, M. Yoshizawa, S. Chiashi, H. Mo Lee, T. Tanaka, H. Kataura, I. Jeon, Y. Matsuo, S. Maruyama, *Chem. Mater.* **2020**, 32, 5125.
- [196] I. Jeon, S. Zeljkovic, K. Kondo, M. Yoshizawa, Y. Matsuo, *ACS Appl. Mater. Interfaces* **2016**, 8, 29866.
- [197] Y. Matsuo, H. Okada, Y. Kondo, I. Jeon, H. Wang, Y. Yu, T. Matsushita, M. Yanai, T. Ikuta, *ACS Appl. Mater. Interfaces* **2018**, 10, 11810.
- [198] D. Zhu, G. Xu, M. Barnes, Y. Li, C.-P. Tseng, Z. Zhang, J.-J. Zhang, Y. Zhu, S. Khalil, M. M. Rahman, R. Verduzco, P. M. Ajayan, *Adv. Funct. Mater.* **2021**, 31, 2100505.
- [199] X. Li, H. Wang, Z. Chen, H.-S. Xu, W. Yu, C. Liu, X. Wang, K. Zhang, K. Xie, K. P. Loh, *Adv. Mater.* **2019**, 31, 1905879.
- [200] X. Chen, Y. Xu, F.-H. Du, Y. Wang, *Small Methods* **2019**, 3, 1900338.
- [201] K. Amin, N. Ashraf, L. Mao, C. F. J. Faul, Z. Wei, *Nano Energy* **2021**, 85, 105958.
- [202] W. Lyu, W. Zhang, H. Liu, Y. Liu, H. Zuo, C. Yan, C. F. J. Faul, A. Thomas, M. Zhu, Y. Liao, *Chem. Mater.* **2020**, 32, 8276.
- [203] W. Lyu, C. Yan, Z. Chen, J. Chen, H. Zuo, L. Teng, H. Liu, L. Wang, Y. Liao, *ACS Appl. Energy Mater.* **2022**, 5, 3706.
- [204] D. D. Chronopoulos, H. Saini, I. Tantis, R. Zbořil, K. Jayaramulu, M. Otyepka, *Small* **2022**, 18, 2104628.
- [205] X. Hu, T. Huang, S. Wang, S. Lin, Z. Feng, L.-H. Chung, J. He, *Electrochim. Acta* **2021**, 398, 139317.
- [206] X. Qian, F. Li, L. Jin, *Microporous Mesoporous Mater.* **2022**, 329, 111558.
- [207] Y. Qiao, H. Zhang, Y. Hu, W. Li, W. Liu, H. Shang, M. Qu, G. Peng, Z. Xie, *Int. J. Miner. Metall. Mater.* **2021**, 28, 1611.
- [208] Y. Xu, S. Hou, G. Yang, T. Lu, L. Pan, *J. Solid State Electrochem.* **2018**, 22, 785.
- [209] J. Ren, X. Yang, J. Yu, X. Wang, Y. Lou, J. Chen, *Sustainable Energy Fuels* **2020**, 4, 6105.
- [210] D. Wang, G. Zheng, W. Zhang, X. Niu, J. Yan, T. Nie, Z. Ji, Y. Gu, X. Yan, *J. Alloys Compd.* **2021**, 881, 160496.
- [211] I. Pochorovski, H. Wang, J. I. Feldblyum, X. Zhang, A. L. Antaris, Z. Bao, *J. Am. Chem. Soc.* **2015**, 137, 4327.



Yong Jun Choi is now pursuing his bachelor's degree under the supervision of Prof. Il Jeon at the SKKU Advanced Institute of Nano Technology (SAINT) in Sungkyunkwan University (SKKU), South Korea. His main interest is the synthesis of dispersant for carbon nanotubes.



Edric John Cruz Nacpil earned his Ph.D. in mechanical engineering from the University of Tokyo, Japan in 2020. He conducted research in artificial intelligence (AI) for 3 years as a senior researcher at Corp & Co., Inc., Japan. He then founded Azukipan IT Solutions, a startup in Japan specializing in innovative web and mobile application development. He is concurrently investigating AI applications as a postdoctoral researcher at the SKKU Advanced Institute of Nano Technology in Sungkyunkwan University, South Korea. His research focuses on AI development to improve solar cell efficiency and the robustness of optoelectronic sensing for autonomous vehicles.



Jiye Han received the M.S. and Ph.D. degrees in Nano Fusion Technology from Pusan National University in 2022. She was a researcher at the University of Tokyo. And now she is a researcher professor at the Sungkyunkwan University Advanced Institute of Nano Technology (SAINT) in Sungkyunkwan University (SKKU), South Korea. Her research interests include the fabrication of structures based on biomaterials and nanoscale materials, such as nanocarbons and nanoparticles, and their application in photovoltaic devices.



Ick Soo Kim received his Ph.D. degree from Nagoya University in 2000, and now he is a distinguished professor at Shinshu university, Japan. He is one of the distinguished professors for Soochow University, China and adjunct professor of POSTECH, Korea. His research focuses on design and synthesis of electrospun nanofibers and its nanocomposites for various applications. Also, his work focused on the development of transition metal-based heterogeneous nanocatalysts for organic transformations.



Il Jeon read chemistry for Bachelors and Masters degrees at Oxford University, UK. Upon graduation in 2008, he worked as the youngest senior researcher at LG Display Co. Ltd., South Korea for 5 years. In 2016, he received a Ph.D. degree in chemistry with honors from the University of Tokyo, Japan. After working as a JSPS postdoctoral fellow, he worked as an assistant professor and a lecturer at the same university. He later joined Sungkyunkwan University (SKKU) as an associate professor in the Department of Nano Engineering and SKKU Advanced Institute of NanoTechnology (SAINT). Currently, he serves as the vice provost for International Affairs at SKKU while holding an early-tenured professorship. His team are working on nanomaterials, namely, nanocarbon and biomaterials for various devices ranging from energy (solar cells and batteries) to sensor applications. Additionally, he is the founder and CEO of JLabNT Co. Ltd.